41540R04

KINETICS OF SLURRY PHASE FISCHER-TROPSCH SYNTHESIS

Fourth Annual Technical Progress Report

Reporting Period Start Date: 10/01/2005

Reporting Period End Date: 09/30/2006

Report prepared by:

Dr. Dragomir B. Bukur (Professor, PI)

Contributors:

Dr. Gilbert F. Froment (Research Professor, Co-PI)

Tomasz Olewski (MSc., Research Technician)

Department of Chemical Engineering
Texas A&M University
College Station, TX 77843-3122

Date Report was issued: March 26, 2007

Grant No. DE-FG26-02NT41540

Texas A&M University
1260 TAMU
College Station, TX 77843-1260

Prepared for

U.S. Department of Energy
University Coal Research Program
National Energy Technology Laboratory
Project Officer: Robert M. Kornosky

Disclaimer

Abstract

This report covers the fourth year of a research project conducted under the University Coal Research Program. The overall objective of this project is to develop a comprehensive kinetic model for slurry-phase Fischer-Tropsch synthesis (FTS) employing iron-based catalysts. This model will be validated with experimental data obtained in a stirred-tank slurry reactor (STSR) over a wide range of process conditions. The model will be able to predict molar flow rates and concentrations of all reactants and major product species (water, carbon dioxide, linear 1- and 2-olefins, and linear paraffins) as a function of reaction conditions in the STSR.

During the fourth year of the project, an analysis of experimental data collected during the second year of this project was performed. Kinetic parameters were estimated utilizing product distributions from 27 mass balances. During the reporting period two kinetic models were employed: a comprehensive kinetic model of Dr. Li and co-workers (Yang et al., 2003) and a hydrocarbon selectivity model of Van der Laan and Beenackers (1998, 1999)

The kinetic model of Yang et al. (2003) has 24 parameters (20 parameters for hydrocarbon formation, and 4 parameters for the water-gas-shift (WGS) reaction). Kinetic parameters for the WGS reaction and FTS synthesis were estimated first separately, and then simultaneously. The estimation of these kinetic parameters employed the Levenberg-Marquardt (LM) method and the trust-region reflective Newton large-scale (LS) method. A genetic algorithm (GA) was incorporated into estimation of parameters for FTS reaction to provide initial estimates of model parameters.

All reaction rate constants and activation energies were found to be positive, but at the 95% confidence level the intervals were large. Agreement between predicted and experimental reaction rates has been fair to good. Light hydrocarbons are predicted fairly accurately, whereas the model underpredicts values of higher molecular weight hydrocarbons.

Van der Laan and Beenackers hydrocarbon selectivity model provides a very good fit of the experimental data for hydrocarbons up to about $C_{20.}$ However, the experimental data shows higher paraffin formation rates in C_{12}-C_{25} region which is likely due to hydrocracking or other secondary reactions. The model accurately captures the observed experimental trends of decreasing olefin to paraffin ratio and increasing α (chain growth length) with increase in chain length.

TABLE OF CONTENTS

Introduction

The overall objective of this project is to develop a comprehensive kinetic model for slurry-phase Fischer-Tropsch synthesis (FTS) employing iron-based catalysts. This model will be validated with experimental data obtained in a stirred-tank slurry reactor (STSR) over a wide range of process conditions. This model will be able to predict concentrations of all reactants and major product species (water (H_2O), carbon dioxide (CO_2), linear 1- and 2-olefins, and linear paraffins) as a function of reaction conditions in the STSR. The kinetic model will be useful for preliminary reactor design and process economics studies. The overall program is divided into four tasks. A brief description and schedule for each task is provided in the following:

Task 1. Development of Kinetic Models (November 1, 2002 - March 31, 2006)

Kinetic models will be formulated utilizing the current state-of-the-art understanding of reaction mechanisms for the formation of reaction intermediates and hydrocarbon products. Models will be based on adsorption/desorption phenomena for reactants and product species. These models will be continually updated on the basis of experimental data obtained in Task 3, and subsequent data analysis conducted in Task 4.

Task 2. Catalyst Synthesis (August 1, 2003 - October 30, 2003)

A precipitated iron (Fe) catalyst with nominal composition 100 Fe/3 Cu/4 K/16 SiO_2 (in parts per weight; Cu = copper; K = potassium; SiO_2 = silica) will be synthesized utilizing equipment and procedures developed in the laboratory at Texas A&M University (TAMU). As an alternative, a robust commercially available catalyst with similar performance characteristics to the TAMU catalyst may be utilized.

Task 3. Experiments in a Stirred Tank Slurry Reactor (January 15, 2003 - March 31, 2004)

Experiments will be conducted in a 1 dm^3 (1 dm^3 = 1 liter = 1 L) stirred tank slurry reactor (STSR) over a wide range of process conditions of industrial significance. Synthesis gas (syngas) feed hydrogen (H_2) to carbon monoxide (CO) molar ratio will vary from 0.67 (coal-derived syngas) to 2 (natural gas-derived syngas). Baseline conditions will be repeated periodically to assess the extent of catalyst deactivation.

Task 4. Model Discrimination and Parameter Estimation (March 1, 2005 – November 30, 2006)

The Langmuir-Hinshelwood-Hougen-Watson (LHHW) approach and the concept of rate limiting step result in a large number of competing kinetic models. Discrimination between the rival models will be based upon the quality of fit, supplemented with statistical tests on parameter values and the physicochemical meaningfulness of the estimated parameter values.

Current Status

Task 1. Development of Kinetic Models

The work on this task was initiated in June 2004. The initial work focused on adoption of one of the kinetic models of Lox and Froment (1993a, 1993b) to a stirred-tank slurry reactor. The kinetic models of Yang et al. (2003) and Van der Laan and Beenackers (1998, 1999) were also utilized to analyze the experimental data.

Task 2. Catalyst Synthesis

Instead of synthesizing a new batch of precipitated catalyst (100 Fe/3 Cu/4 K/16 SiO_2 (in parts by weight), we used a precipitated iron catalyst prepared by Ruhrchemie AG (Oberhausen-Holten, Germany). This catalyst (LP 33/81), having a nominal composition 100 Fe/4.3 Cu/4.1 K/25 SiO_2 (in parts by weight), was used initially in fixed-bed reactors at Sasol in South Africa. It has been tested extensively at TAMU (Bukur *et al*., 1990; Zimmerman and Bukur, 1990; Zimmerman *et al.*, 1992; Bukur *et al*., 1995), and was used in a previous study of the kinetics of FTS by Lox and Froment (Lox and Froment, 1993a, 1993b). The LP 33/81 catalyst is robust and has a selectivity that is similar to the TAMU catalyst.

Task 3. Experiments in a Stirred-Tank Slurry Reactor

Three tests (Runs SB-21903, SB-26203 and SB-28603) with the Ruhrchemie catalyst were conducted in a 1 dm^3 stirred-tank slurry reactor (Autoclave Engineers) over a wide range of process conditions. The reaction temperature was 220, 240 or 260°C, the pressure varied from 0.8 to 2.5 MPa, the synthesis gas feed H_2/CO molar ratio was either 2/3 or 2, and the gas space velocity (SV) under the normal (standard) conditions (273.15°K, 101325 Pa) varied from 0.52 to 23.5 $Ndm^3\ g_{Fe}^{-1}\ h^{-1}$ to obtain wide range of conversions. The results and qualitative analysis were described in detail in the Second Annual Report for this project (Bukur et al., 2005).

Task 4. Model Discrimination and Parameter Estimation

A method to calculate vapor-liquid-equilibrium (VLE) in the STSR was developed. Results were discussed in the Third Annual Report for this project (Bukur et al., 2006). The estimated kinetic parameters from the experimental data in the STSR were calculated using the kinetic models of Lox and Froment (1993b), Yang et al. (2003), and Van der Laan and Beenackers (1998, 1999). The results of the estimation of kinetic parameters are described in the Results and Discussion Section of this report.

Experimental

Three tests (Runs SB-21903, SB-26203 and SB-28603) were conducted in a 1 dm^3 stirred-tank slurry reactor (Autoclave Engineers). A schematic of the experimental apparatus is shown in Figure 1. The feed gas flow rate was adjusted with a mass flow controller and passed through a series of oxygen removal, alumina, and activated charcoal traps to remove trace impurities. After leaving the reactor, the exit gas passed through a series of high and low (ambient) pressure traps to condense the liquid products. High molecular weight hydrocarbons (wax), withdrawn from a slurry reactor through a porous cylindrical sintered metal filter, and liquid products, collected in the high and low pressure traps, were analyzed by capillary gas chromatography (Varian 3400 gas chromatograph). Liquid products collected in the high and atmospheric pressure traps were first separated into an organic phase and an aqueous phase and then analyzed using different columns and temperature programmed methods (Varian 3400 gas chromatograph). The reactants and noncondensible products leaving the ice traps were analyzed whith an on-line gas chromatograph (Carle AGC 400) with multiple columns using both flame ionization and thermal conductivity detectors. A schematic of the product analysis procedure is shown in Figure 2. Further details on the experimental set up, operating procedures, and product quantification can be found elsewhere (Bukur *et al*., 1990; Zimmerman and Bukur, 1990; Bukur *et al*., 1994; Bukur *et al*., 1996).

The Ruhrchemie catalyst (15 g in Run SB-21903, 11.2 g in Run SB-26203, and 25 g in Run SB-28603) was calcined in air at 300°C and a sample with a size fraction between 140-325 mesh was loaded into the reactor filled with 300-320 g of Durasyn 164 oil (a hydrogenated 1-decene homopolymer, ~ C_{30}). The catalyst was pretreated in CO at 280°C, 0.8 MPa (100 psig),

and 3 NL/g-cat/h (where, NL/h, denotes volumetric gas flow rate at 0°C and 1 bar) for 12 hours. After the pretreatment, the catalyst was tested initially at 260°C, 1.5 MPa (200 psig), 4 NL/g-Fe/h using CO-rich synthesis gas (H_2/CO molar feed ratio of 2/3). After reaching a stable steady-state value (~60 h on stream), the catalyst was tested at different process conditions. The minimum length of time between changes in process conditions was 20 h.

Results and Discussion

Kinetic parameter estimation was made utilizing experimental data from 27 sets of process conditions. These conditions are summarized in Table 1. Three kinetic models from the literature have been adopted to analyze the experimental data from the STSR. Two kinetic models (Lox and Froment, 1993b; Yang et al., 2003) provide a complete product distribution (inorganic species and hydrocarbons) whereas the kinetic model of Van der Laan and Beenackers (1998, 1999) can be used to predict hydrocarbon product distribution only.

Lox and Froment Model

This model was previously described in the Third Annual Report for this project (Bukur et al., 2006), but is included here for completeness.

The model reported as the best by Lox and Froment (marked by symbol ALII in Lox and Froment, 1993b) for their operating conditions (high H_2/CO feed ratio of 3) has been selected for the initial estimation of kinetic parameters from the experimental data in the STSR. It accounts for formation of carbon dioxide, water, paraffins, and total olefins (it does not distinguish between 1- and 2-olefins) as well as consumption of hydrogen and water. This model predicts a constant value for the chain growth probability factor, α, however TAMU experimental data (Bukur et al., 2005) show that α is not constant (i.e. it varies with carbon number). A simplified form of this model contains only five parameters at isothermal conditions. Because of its relative simplicity, this model is well suited for initial studies where the main goal is to learn techniques for parameter estimation and statistical analysis of estimated values of model parameters. The same techniques and computer codes were used in the analysis of other kinetic models.

The ALII model utilizes the LHHW approach and the concept of rate-determining steps (RDS). The elementary steps (reactions) for FTS and WGS reaction are shown in Tables A-1 and A-2, respectively. Reactant molecules are adsorbed on two types of active sites, one for FTS and

the second for WGS reaction, where the surface reactions take place. The model assumes the following two RDS in each path of formation of paraffins and olefins in the Fischer-Tropsch reaction:

- adsorption of carbon monoxide (HC1) and desorption of the paraffin (HC5) in the reaction path leading to the paraffins,
- adsorption of carbon monoxide (HC1) and desorption of the olefin (HC6) in the reaction path leading to the olefins,

and the following one RDS for the WGS reaction path:

- reaction of an adsorbed carbon monoxide with adsorbed hydroxyl group (WGS2; Table A-2).

All relevant equations are given in Appendix A of this report.

Parameter Estimation Methodology

A simplified ALII model of Lox and Froment (1993b) has five kinetic parameters, three for the FTS reaction:

- adsorption of carbon monoxide, $k_{\mathrm{CO,HC}}$,

- desorption of a paraffin, $k_{\mathrm{t,p}}$,

- desorption of an olefin, $k_{\mathrm{t,o}}$,

and two parameters for the WGS reaction:

- constant containing the WGS rate constant $k_{\nu}^{'}$.
- ratio of adsorption constants K_{ν}.

In equations (A.1) to (A.4) the unknowns are five kinetic constants, whereas partial pressures of hydrogen, carbon monoxide, carbon dioxide, and water are known from the VLE calculations ($p_i = y_i \cdot P$).

Parameters are estimated by minimizing an objective function, S. An objective function that minimizes the sum of squares of residuals of reaction rates was used:

$$S = \sum_{h=1}^{v} \sigma_{h,h} \cdot \sum_{i=1}^{n} \left(\hat{R}_{i,h} - R_{i,h} \right)^2 \qquad (1)$$

where $\hat{R}$ means experimental, R represents calculated reaction rate, and $\sigma_{h,h}$ are diagonal elements of the inverse of the error covariance matrix. When replicate experiments are available the weighting factors can be calculated (Froment and Bischoff, 1990) as:

$$\sigma_{h,h} = \left(\frac{\sum_{i=1}^{n_e} \left(\hat{R}_{i,h} - \overline{R}_h \right)^2}{n_e - 1} \right)^{-1} \tag{2}$$

where $\overline{R}_h$ represents the average value of response h over n_e replicate experiments (n_e is equal to 3 in our case), n is a number of experiments at constant temperature, and v is a number of components (in this case: CO, CO_2, H_2, H_2O, twenty n-paraffins $C_{1\text{-}20}$, fourteen 1-olefins $C_{2\text{-}14}$ and pseudo-component $C_{21\text{-}50}$). The reaction rate of pseudo-component C_{21}^{+} is calculated as follows:

$$R_{21+} = \sum_{i=21}^{50} R_i \tag{3}$$

When there is insufficient information about the nature of errors in experimental measurements, another weighting factor can be used. In such cases, the simplest form of the weighting factor is the inverse of squared mean response of the j^{th} variable (Englezos and Kalogerakis, 2001):

$$\sigma_{j,j} = \left(\frac{1}{n} \cdot \sum_{i=1}^{n} \hat{R}_{ij} \right)^{-2} \tag{4}$$

When the weighting factors are not used in equation (1) then the σ matrix is the identity matrix, i.e. $\sigma_{h,h} = 1$.

Minimization of the objective function was done by the Levenberg-Marquardt (LM) method (Marquardt, 1963) which is an improved form of the Newton-Gauss optimization technique. The minimization procedure consists of the following steps:

1. Initial guess of unknown parameters k^0 is made. The corresponding reaction rates are calculated using the assumed values of kinetic parameters and the objective function is evaluated.

2. New (improved) values of kinetic parameters k^i are found by the LM method.
3. New values of reaction rates and the objective function are obtained.
4. If the current (new) value of the objective function is smaller or equal to the previous (old) one then go to Step 5. If not, go to Step 2 and keep iterating until a criterion for minimization is achieved, i.e.:

$$S\left(k^{i+1}\right) \leq S\left(k^{i}\right)$$

5. Stop iterations when the difference between the current and the previous value of the objective function is smaller than the desired convergence criterion, ε_p.

$$\left|S\left(k^{i+i}\right) - S\left(k^{i}\right)\right| \leq \varepsilon_p$$

If the convergence is not achieved, go back to Step 2 and iterate until the convergence criterion is achieved. The numerical value of ε_p is set to 10^{-6}.

Results from Parameter Estimation

Estimated values of kinetic parameters obtained using the objective function (Equation (1)) with weighting factors equal to one and with weighting factors calculated using Equation (4) are shown in Table 2. As can be seen from this table, the rate constant for olefin formation, $k_{t,0}$, estimated assuming that all weighting factors are equal to one, is negative for data at 220°C and 260°C. Therefore, this approach ($\sigma_{h,h} = 1$ in equation (1)) yields unsatisfactory results. The use of weighting factors calculated from Equation (4) results in positive values for all five rate constants at all three temperatures (Table 2).

Statistical parameters associated with calculated rate constants are shown in Table 3. Approximate 95% confidence intervals for the WGS kinetic parameters $k_v^{'}$ and K_v show that these parameters are not significantly different from zero (lower 95% confidence interval gives negative values), whereas the mean values of the three kinetic parameters for the FTS are statistically reliable.

Representative parity plots, for a reaction temperature of 260°C, are shown in Figures 3 and 4. These figures show a comparison of calculated and experimental reaction rates. Calculated and experimental rates for inorganic species (H_2, CO, CO_2, and H_2O) are shown in Figure 3, whereas the results for hydrocarbons are shown in Figure 4. In the case of H_2 and CO, the absolute rates are shown in Figure 3. If the model fits the data, experimental points would lie

on a straight line with a slope of 45°. However, almost all of the calculated reaction rates are smaller then the experimental values (Figures 3 and 4). Results for various hydrocarbon species (Figure 4) are shown with two different scales. As can be seen in this figure, the Lox and Froment's (1993b) ALII model does not predict accurately the formation rates of various hydrocarbons (individual species as well as lumped species). Detailed comparison of predicted and experimental formation rates of individual species (C_1-C_{20} n-paraffins, and C_2-C_{15} olefins) is shown in Figure 5. Experimental values are represented by points, whereas solid lines are model predictions. Model predictions are represented by straight lines on a semi-logarithmic plot (log Rate vs. Carbon number) whereas experimental points have curvatures. It can be seen that the model does not predict accurately the observed reaction rates of individual hydrocarbons.

Figure 6 shows carbon number distribution of hydrocarbon products on a semi-logarithmic scale (logarithm of reaction rate of hydrocarbons containing n carbon atoms vs. carbon number). The model yields a straight line, whereas experimental data show nonlinear dependence on carbon number. The model predictions reflect the ideal Anderson-Schulz-Flory (ASF) distribution characterized by a constant value of the chain growth probability factor α, whereas experimental data show that α varies with carbon number.

Predicted and experimental values of olefin to n-paraffin reaction rates (Olefin to paraffin ratio) as a function of carbon number are shown in Figure 7. The model predictions are represented by a horizontal line, whereas experimental values are carbon number dependent. Clearly the model fails to predict the observed experimental trends both qualitatively and quantitatively.

Activation Energies

From estimated values of kinetic parameters at three reaction temperatures (Table 2, with weighting factors from Equation (4)), the corresponding activation energies and frequency factors have been calculated. The adsorption constant for carbon monoxide adsorption $k_{\mathrm{CO,HC}}$, the desorption rate constant of n-paraffins $k_{\mathrm{t,p}}$, the desorption rate constant of olefin $k_{\mathrm{t,o}}$, and the WGS reaction rate constant $k_{\nu}^{'}$ satisfy the Arrhenius equation:

$$k = A_0 \cdot e^{\frac{-E_a}{RT}} \tag{5}$$

where A_0 is a frequency factor, E_a is an activation energy, R is universal gas constant equal to *8.3144 kJ/mol*, and T is temperature measured in *Kelvin*.

Numerical values of activation energies (E_a) are shown in Table 4. Statistical parameters shown in Table 4 are calculated for one degree of freedom ($n - p$, where n is number of independent values, data at temperatures: 220, 240 and 260°C, whereas p is a number of parameters, A_0 and E_a) and for statistical significance α equal to 0.05. Approximate 95% confidence intervals are large, due to the fact that there is only one degree of freedom in the estimation. However, the approximate confidence intervals indicate that estimated values of activation energies for carbon monoxide adsorption $E_{CO,HC}$, n-paraffin formation $E_{t,p}$, and olefin formation $E_{t,o}$ are reliable, because they are all non-negative. The approximate confidence intervals for the WGS activation energy E_v range from -585 to 1003. This means that the estimated value for E_v (209 kJ/mol) is not significantly different from zero, and it has a small impact on the model result. The relatively small standard error value and high t-value imply that estimated parameter value is obtained with good accuracy. As can be seen, these conditions are satisfied for activation energies: $E_{CO,HC}$, $E_{t,p}$ and $E_{t,o}$.

Activation energies for the formation of paraffins ($E_{t,p}$) and olefins ($E_{t,o}$) can be compared with the corresponding values reported in the literature (Table 5). Reported values of the activation energy for the paraffin formation are between *70* and *112 kJ/mol*, and those for the olefin formation are *97 – 132 kJ/mol*. Activation energies from the TAMU data with the ALII kinetic model of Lox and Froment (1993b) are *121 kJ/mol* for paraffin formation, and *54 kJ/mol* for the olefin formation. The former is slightly higher than the upper bound from the literature, whereas the olefin formation activation energy value is about 50% lower than a typical value from the literature. The estimated activation energy for the WGS reaction (*209 kJ/mol*) is too high when compared to the corresponding values in the literature (*28-137 KJ/mol*), and is not reliable as discussed previously (lower 95% confidence interval gives negative value).

Multi-Response Objective Function *S*

The following objective functions have been used in all subsequent estimations of kinetic parameters. The objective function S_1 utilizes reaction rates R_i and the weighting factor σ.

$$S_1 = \sum_{h=1}^{N_{resp}} \sigma_{h,h}^{-1} \cdot \sum_{i=1}^{N_{\exp}} \left(\hat{R}_{i,h} - R_{i,h}\right)^2 \tag{6}$$

where h is a response that represents a component: CO, CO_2, H_2, H_2O, twenty paraffins $C_{1\text{-}20}$, nineteen olefins $C_{2\text{-}20,}$ and lumped-component $C_{21\text{-}50}$, which gives 40 responses (components); N_{exp} (27) is a number of experiments, and $\sigma_{h,h}^{-1}$ are diagonal elements of the inverse of the error covariance matrix.

The objective function, S_2, utilizes molar flow rates of individual components

$$S_2 = \sum_{j=1}^{N_{resp}} \sum_{i=1}^{N_{\exp}} W_i \cdot \left(\frac{m_{i,j,\exp} - m_{i,j,cal}}{m_{i,j,\exp}} \right)^2 \tag{7}$$

where $m_{i,j}$ is molar flow rate of jth component in ith experiment, and W_i is the weighting factor.

The accuracy of the fitted model relative to the experimental data was obtained from the mean absolute relative residual (MARR) function:

$$MARR = \frac{1}{N_{resp} N_{\exp}} \sum_{i=1} \sum_{j=1} \left| \frac{\hat{R}_{i,j} - R_{i,j}}{R_{i,j}} \right| \tag{8}$$

A statistical test for the kinetic model is measured either by the F-value or by correlation coefficient. The statistics for the estimate parameters are expressed by either t-value or the 95% confidence interval.

An analysis of residuals of estimates has been done utilizing the relative residual (RR) which is defined as follows:

$$RR_{i,j} = 100 \cdot \frac{\hat{R}_{i,j} - R_{i,j}}{R_{i,j}} \tag{9}$$

where i represents the component, j represents the experiment, and R and $\hat{R}$ are the experimental and calculated reaction rates, respectively.

The total olefin (1- and 2-olefin) to paraffin ratio as well as 2-olefin to total olefin ratio (for hydrocarbons with i carbon atoms) are defined as follows:

$$\text{Total Olefin to Paraffin Ratio}_\text{i} = \frac{\text{Total Olefin Rate}_\text{i}}{\text{Paraffin Rate}_\text{i}} \tag{10}$$

$$2^{-}\text{Olefin to Total Olefin Ratio}_\text{i} = \frac{2^{-}\text{Olefin Rate}_\text{i}}{\text{Total Olefin Rate}_\text{i}} \tag{11}$$

Kinetic Model of Li and co-workers

This model was proposed by Dr. Li's group at the Institute of Coal Chemistry of Chinese Academic of Science in Taiyuan, PR China (Yang et al., 2003).

Main features of the model are as follows:

- olefin readsorption is included,
- separate kinetic reaction rate constant is used for methane,
- solution of hydrocarbon formation reaction rates requires the numerical solution of a set of two non-linear algebraic equations,
- model predicts that olefin to paraffin ratio is a function of carbon number.

Elementary reactions and final equations for this model are given in Appendix B. The total number of parameters that need to be estimated is 24 (20 parameters for hydrocarbon formation, and 4 parameters for the WGS reaction). Kinetic parameters for the WGS reaction and FTS synthesis were estimated first separately, and then simultaneously.

Estimation of Parameters for WGS Reaction

The WGS reaction model is described as one equation for carbon dioxide formation (Equation B.12). This model contains four parameters (two for the reaction rate constant k_V and two for the adsorption equilibrium constant K_V). It can be noted that the constant K_V is a ratio of adsorption constants (Equation B.13). Kinetic parameters were estimated using a trust-region reflective Newton large-scale (LS) method (Coleman and Li, 1994, 1996). Results are given in Table 6. The grey-colored cells in Table 6 represent results obtained with the objective function S_1 whereas the results in cells without color were obtained using the objective function S_2. The objective function S_2 (relative objective function) gives a better fit, measured by MARR (~20% vs. 26% using S_1). Obtained activation energy values for CO_2 formation are in range 60 – 95 kJ/mol whereas values for enthalpy change, which represents the difference of two enthalpy change values (therefore it can be negative), are between -46 and – 80 (kJ/mol).

Although fitting of the model gives good statistics values in all cases (F-value ~30 – 60 and correlation coefficient ~0.64 – 0.91), the estimated parameters have large confidence intervals ranging from negative to large positive values. A parity plot, calculated vs. experimental reaction rate of carbon dioxide formation, is shown in Figure 8. It can be seen that the calculated values are nearly constant for a particular temperature (4 low points are at 220^{o}C, 8 points in the middle are for 240^{o}C, and 15 upper points are for 260^{o}C). This shows that the

model predicts that the WGS reaction rate is proportional to the reaction rate constant ($R_{CO2} \sim k_V$).

In order to check if these results represent a global minimum, a genetic algorithm (GA) has been incorporated into the estimation procedure (Goldberg, 1989, Conn et al., 1997). A hybrid method: GA first, followed by the Levenberg-Marquardt (LM) or LS method was employed. The GA method finds a good initial guess close to the global minima, and LM or LS provides more precise values. Results are shown in Table 7. The grey-colored cells in the table represent results from the GA method whereas cells that are not colored are results from either LM or LS method. The GA method has found two global minima (grey cells, rows W17 and W20), which have different values of parameters. These values were used as initial guesses for the LM and LS methods. The activation energy obtained is between 128 and 143 kJ/mol whereas the difference of enthalpy change varies from 6 to -12. It can be seen that applying a hybrid method gives similar statistics for fitting of the model (~33, 20 and 0.65 for F-value, MARR and correlation coefficient, respectively), but it gives a narrow confidence interval for the activation energy (lower 95% confidence interval limit is positive). For case W18 in Table 7, the activation energy is 143.5 kJ/mol and its confidence interval is 95 – 192 kJ/mol. The parity plot for carbon dioxide (Figure 9) shows better agreement between model predictions and experimental data, than that obtained using the LM or LS method directly.

It can be noted that both the LM and LS methods give the same result (Table 7, W18 and W19, respectively), but the LM method converges much faster (only 26 iterations, compared to 131 for the LS). It seems that a combination of the GA method followed by the LM method is better, and very effective for estimation of kinetic parameters. This confirms that the LM is a good searching method provided it has a good starting point.

Estimation of Parameters for FTS Reaction

The Fischer-Tropsch synthesis reaction model (hydrocarbons rate formation) contains 20 unknown parameters. Calculation of rates for every set of parameters (i.e. for every iteration) requires numerical solution of two non-linear algebraic equations (Equations. B.4 and B.11).Parameters were estimated using the objective function S_2 (with $W_i = 1$) and a trust-region reflective Newton large-scale method (LS). Results are shown in Table 8.

A significant value of F for the model was obtained (about 15). In addition, a relatively narrow 95% confidence interval for all activation energies was obtained. However, the degree of agreement between experimental and calculated responses, measured by MARR, is relatively large (~65%) and the correlation coefficient is small (~0.15). A parity plot for methane, ethane, and ethene is shown in Figure 10, whereas the results for hydrocarbon groups $C_{3\text{-}10}$ and $C_{11\text{-}20}$ are shown in Figure 11. It can be seen that the model provides good fit for light paraffins and all olefins, whereas the calculated $C_{11\text{-}20}$ paraffins are significantly smaller than the corresponding experimental values. Paraffin and olefin rates as a function of carbon number are shown in Figures 12 and 13 (for all mass balances). Again, good agreement was obtained between calculated and experimental values for light paraffins and olefins for most mass balances.

Simultaneous Estimation of Kinetic Parameters

This is a multi-response estimation of all species: carbon dioxide (WGS), hydrocarbons (FTS), and inorganic species (hydrogen, carbon monoxide, and water). Rates for hydrogen, carbon monoxide and water were calculated based on stoichiometry (Equations A.6, A.7 and A.8, respectively). This approach considers 24 parameters. The results from WGS and FTS estimations were used as initial guesses in this estimation.

The use of a multi-response estimation did not result in the improvement of model parameters. Both minimization methods, LM and LS, lead to minor changes in values of pre-exponential factors (mostly for WGS) and do not result in improvement of other parameters. Figure 14 is a parity plot for inorganic components: carbon monoxide, hydrogen, carbon dioxide, and water. Almost all calculated rates are smaller than experimental ones. Predicted rates for carbon dioxide formation are not as good as those obtained from the WGS estimation alone (Figures 8 and 9 vs. Figure 14).

Hydrocarbon selectivity Model of Van der Laan and Beenackers

Van der Laan and Beenackers (1998, 1999) developed so-called olefin readsorption product distribution model (ORPDM) for formation of hydrocarbons in FTS. Reaction network of hydrocarbon formation for this model is presented in Appendix C (Figure C-1). Chain growth initiates by hydrogenation of an adsorbed monomer ($^{*}CH_2$) to an adsorbed methyl group ($^{*}CH_3$). Chain propagation occurs via insertion of an adsorbed monomer into an adsorbed alkyl species

($^{*}C_nH_{2n+1}$), which can terminate to either n-paraffin (C_nH_{2n+2}) by hydrogenation or to olefin (C_nH_{2n}) by dehydrogenation (i.e. hydrogen abstraction). According to this reaction network olefin readsorption leads to adsorbed alkyl species, which can either propagate or terminate. Elementary reactions for this model are shown in Table C-1, and detailed derivation of kinetic equations is given in Appendix C.

Parameters were estimated from experimental data at constant temperature. There are three sets of experimental data at temperatures 220, 240 and 260°C, which include 4, 8 and 15 mass balances, respectively.

Parameters were estimated using objective function S_1, defined by Equation (6) and the LM method. Total number of experiments, $N_{\exp}$, is 4, 8, or 15 at 220, 240 and 260°C, respectively, whereas number of responses, N_{resp}, is 40 ($C_{1\text{-}20}$ paraffins, $C_{2\text{-}20}$ olefins, and pseudo-component $C_{21\text{-}50}$). Degrees of freedom for all of these three cases are high and equal to 137, 277, and 522 for temperatures of 220, 240, and 260°C.

Van der Laan and Beenackers model (1998, 1999) has 8 parameters (for every set of process conditions). These parameters are related to the following steps: initiation (κ_1), propagation (κ_p), methane formation ($\kappa_{t,p}^{(1)}$), ethane formation ($\kappa_{t,p}^{(2)}$), olefin formation ($\kappa_{t,o}$), ethylene readsorption ($\kappa_{r,o}^{(2)}$), readsorption of C_3^+ olefins ($\kappa_{r,o}$), and solubility/physiosorption dependence of olefin with carbon number (c). The pseudo-kinetic parameters are related to the true kinetic parameters and surface coverages of the reaction intermediates as follows:

$$\kappa_1 = k_{p1} \cdot \theta_{CH_2,s_1} \cdot \theta_{H,s_1}$$

$$\kappa_p = \frac{k_p \cdot \theta_{CH_2,s_1}}{k_{t,p} \cdot \theta_{H,s_1}}$$

$$\kappa_{t,p}^{(1)} = \frac{k_{t,p}^{(1)}}{k_{t,p}}$$

$$\kappa_{t,p}^{(2)} = \frac{k_{t,p}^{(2)}}{k_{t,p}} \qquad (12)$$

$$\kappa_{t,o} = \frac{k_{t,o} \cdot \theta_{s_1}}{k_{t,p} \cdot \theta_{H,s_1}}$$

$$\kappa_{r,o}^{(2)} = k_{r,o}^{(2)} \cdot \theta_{s_1} \cdot \theta_{H,s_1} \cdot \frac{R_g \cdot T}{SV}$$

$$\kappa_{r,o} = k_{r,o} \cdot \theta_{s_1} \cdot \theta_{H,s_1} \cdot \frac{R_g \cdot T}{SV}$$

where θ is the surface coverage of species (or sites).

Van der Laan and Beenackers (1998, 1999) found that parameters $\kappa_{t,p}^{(1)}$, $\kappa_{t,p}^{(2)}$, $\kappa_{r,o}^{(2)}$, and c are constant at a given temperature (250°C). From the above definitions and Appendix C, one can see that only two parameters, $\kappa_{t,p}^{(1)}$ and $\kappa_{t,p}^{(2)}$, represent ratios of two true kinetic constants and thus are expected to be dependent on temperature only. Also, parameter *c* can be constant at a given temperature. This parameter is related to non-intrinsic effects on reaction rates, such as intraparticle diffusivion, physisorption and/or solubility. However, it must be noted that $\kappa_{r,o}^{(2)}$ parameter is expected to be a function of process conditions (gas space velocity, and surface concentrations of intermediates, which in turn are expected to vary with P, T, SV, and/or H_2/CO feed ratio). Two types of estimation for $\kappa_{r,o}^{(2)}$ parameter: (a) temperature dependent only; and (b) dependent on all conditions (i.e. its numerical value is different for each mass balance conducted at different process conditions) were performed.

The first estimation, with $\kappa_{r,o}^{(2)}$ dependent on temperature only (Van der Laan and Beenackers approach) is shown in Table 9. In addition parameters $\kappa_{t,p}^{(1)}$, $\kappa_{t,p}^{(2)}$, and c were also assumed to be dependent on temperature only, whereas the remaining 4 model parameters κ_1, κ_p, $\kappa_{t,0}$, and $\kappa_{r,0}$ were estimated for each set of conditions. As can be seen from Table 9, this assumption leads to negative values of some parameters (highlighted cells). Thus, this approach is not valid for the TAMU experimental data.

Results from the second procedure, $\kappa_{r,o}^{(2)}$ estimated for each set of conditions, are shown in Table 10. The statistics for estimated parameters, t-values, corresponding to this case are shown in Table 11. All parameters, except $\kappa_{t,o}$, $\kappa_{r,o}^{(2)}$, and $\kappa_{r,o}$, are significantly different than zero, and their t-values are greater than one. Moreover most of t-values are quite high (greater then 10), which means that the parameters have a quite narrow 95% confidence interval. However most of parameters related to termination and readsorption of olefins ($\kappa_{t,o}$, $\kappa_{r,o}^{(2)}$, and

$\kappa_{r,o}$) are statistically insignificant (their t-values are smaller then 1 – highlighted cells in Table 11).

Comparison of predicted and experimental reaction rates of n-paraffins and olefins for selected mass balances (6 cases) is shown in Figure 15. In general a good fit has been obtained for paraffins and olefins up to C_{20}. Average mean absolute relative residuals (MARR) values for C_1-C_{20} hydrocarbons are generally smaller then 30%. As shown in Figure,15, the TAMU experimental data often show high paraffin reaction rates in C_{12}-C_{25} carbon number range (a "hump" in experimental data) which may be due to secondary reactions (e.g. hydrocracking). These deviations are not accounted by the present model and result in higher MARR values. Fitting for a pseudo-component (paraffin C_{21}^{+}) is generally worse than that for paraffins and olefins up to C_{20}. In some cases MARR values for C_{21}^{+} showed a very good overall fit, whereas the fit was not so good for individual paraffins (C_{21} to C_{50}).

As pointed out by Van der Laan and Beenackers (1999), a strong correlation between parameters $\kappa_{t,o}$ and $\kappa_{r,o}$ occurs at a high olefin readsorption rate ($\kappa_{r,o} \cdot \exp(c \cdot n) >> 1$). In such a case, these parameters should not be estimated separately, and the $\kappa_{t,o} / \kappa_{r,o}$ ratio should be estimated as one parameter. Correlation between these two parameters results in their non-significant statistical values as mentioned previously for the TAMU experimental data (results shown in Table 11). By combining these two parameters into one, the kinetic model of Van der Lann and Beenackers has 7 parameters (see Appendix C for details). Three of these parameters are temperature dependent only ($\kappa_{t,p}^{(1)}$, $\kappa_{t,p}^{(2)}$ and c) whereas others (κ_1, κ_p, $b^{(2)}$, b) have different values at different process conditions. Estimated parameter values are given in Table 12, and the corresponding t-values in Table 13. Parameter estimation by this method gives much better statistics (t-values) for parameters related to olefin readsorption and termination ($b^{(2)}$, b) while at the same time does not change statistical significance of other model parameters.

The best, median, and worse fitting results for total product distribution, expressed by MARR, are shown in Figure 16. The largest MARR values were obtained for the pseudo-component C_{21}^{+}. It should be noted that one of the reasons for high MARR values are errors in experimental data, and existence of the "hump' in paraffin production rates in C_{12}-C_{25} carbon number range.

Conclusions

During the fourth year of the project, an analysis of experimental data collected earlier (during the second year of this project) was performed. Kinetic parameters were estimated utilizing product distributions from 27 mass balances. During the reporting period two kinetic models were employed: a comprehensive kinetic model of Dr. Li and co-workers (Yang et al., 2003) and a hydrocarbon selectivity model of Van der Laan and Beenackers (1998, 1999).

The kinetic model of Yang et al. (2003) has 24 parameters (20 parameters for hydrocarbon formation, and 4 parameters for the WGS reaction). Kinetic parameters for the WGS reaction and FTS were estimated first separately, and then simultaneously. To accomplish this the Levenberg-Marquardt (LM) method and a trust-region reflective Newton large-scale (LS) method were employed. A genetic algorithm (GA) was incorporated into the estimation of parameters for the FTS reaction to provide initial estimates of model parameters. These values were subsequently used as initial guesses for the LM and/or the LS methods to improve the values.

All reaction rate constants and activation energies are found to be positive, but 95% confidence intervals are large. The agreement between predicted and experimental reaction rates has been fair to good. Light hydrocarbons are predicted fairly accurately, whereas the model underpredicts values of higher molecular weight hydrocarbons. Also, the model does not predict that the chain growth parameter increases with increase in molecular weight.

The Van der Laan and Beenackers hydrocarbon selectivity model provides a very good fit of the experimental data for hydrocarbons up to about C_{20} (with the exception of experimental data that show higher paraffin formation rates in C_{12}-C_{25} region, due to hydrocracking or other secondary reactions). Estimated values of all model parameters (true and pseudo-kinetic parameters) have high statistical significance after combining parameters related to olefin termination ($\kappa_{t,o}$) and readsorption ($\kappa_{r,o}$) into one ($\kappa_{t,o}/\kappa_{r,o}$). The model was found to capture the observed experimental trends of decreasing olefin to paraffin ratio and increasing α (chain growth length) with increase in chain length well.

Future Work

The plan for the remainder of this project (October 1, 2006 – December 31, 2006) is to extend Van der Laan and Beenacker's ORPDM model to include the formation of 2-olefins.

Acknowledgements

This work was supported by the U.S. Department of Energy (University Coal Research Program) under Grant No. DE-FG26-02NT41540.

References

Bukur, D.B., S.A. Patel and X. Lang, *Appl. Catal.*, 61, 329 (1990)

Bukur, D. B., L. Nowicki and X.Lang, , *Chem. Eng. Sci*., 49, 4615 (1994)

Bukur, D. B., L. Nowicki, R. K. Manne and X. Lang, *J. Catal*., 155, 366 (1995)

Bukur, D. B., L. Nowicki and S. A. Patel, *Can. J. Chem. Eng*., 74, 399 (1996)

Bukur D.B., G.F. Froment, L. Nowicki, M. Nyapathi and X. Wang, *"Kinetics of Slurry Phase Fischer-Tropsch Synthesis"*, Second Annual Technical Progress Report for DOE, Contract No. DE-FG26-02NT41540, Texas A&M University, College Station, TX, January 2005

Bukur D.B., G.F. Froment and T. Olewski, *"Kinetics of Slurry Phase Fischer-Tropsch Synthesis"*, Third Annual Technical Progress Report for DOE, Contract No. DE-FG26-02NT41540, Texas A&M University, College Station, TX, January 2006

Coleman, T.F. and Y. Li, *SIAM Journal on Optimization*, Volume 6, 418 (1996)

Coleman, T.F. and Y. Li, *Mathematical Programming*, Volume 67, Number 2, 189 (1994)

Conn, A. R., N. I. M. Gould, and Ph. L. Toint, *Mathematics of Computation*, Volume 66, Number 217, 261 (1997)

Dictor R.A. and A.T. Bell, *J. Catal*., 97:121–36 (1986)

Dry, M. E., T. Shingles, L. J. Boshoff and J. Oosthuizen, *J. Catal.*, 25, 99-104 (1972)

Englezos, P. and N. Kalogerakis, (2001) *"Applied parameter estimation for Chemical Engineers"*, New York: Mercel Dekker, Inc.

Feimer J.L., P.L. Silveston and RT. Huggins, *Ind. Eng. Chem. Prod. Res. Dev*., 20, 609 (1981)

Froment G.F. and Bischoff K.B., (1990) *"Chemical Reactor Analysis and Design"*, Second Edition, New York: John Wiley & Sons, Inc.

Goldberg, David E., Genetic Algorithms in Search, Optimization & Machine Learning, Addison-Wesley, 1989.

Lox, E. S. and G. F. Froment, *Ind. Eng. Chem. Res.*, 32, 61 (1993a)

Lox, E. S. and G. F. Froment, *Ind. Eng. Chem. Res.*, 32, 71 (1993b)

Marquardt, D.W., *J. Soc. Industr. Appl. Math.*, 11, 431 (1963)

Nettelhoff, H., R. Kokuun, S. Ledakowicz and W.D. Decker, *Ger. Chem. Eng.*, 8, 177 (1985)

Van der Laan, G. P. and A. A. C. M. Beenackers, *Stud. Surf. Sci. Catal.*, 119, 179 (1998)

Van der Laan, G. P. and A. A. C. M. Beenackers, *Ind. Eng. Chem. Res.*, 38, 1277 (1999)

Wang Y.-N., W.P. Ma, Y.J. Lu, J. Yang, Y.Y. Xu, H.W. Xiang, Y.W. Li, Y.L. Zhao and B.J. Zhang, *Fuel*, 82, 195-213 (2003)

Yang J., L. Ying, J. Chang, Y.N. Wang, L. Bai, Y.Y. Xu, H.W. Xiang, Y.W. Li and B. Zhong, *Ind. Eng. Chem. Res.*, 42, 21 (2003)

Zimmerman, W. H. and D. B. Bukur, *Can. J. Chem. Eng.*, 68, 292 (1990)

Zimmerman, W. H., *"Kinetic Modeling of the Fischer-Tropsch Synthesis"*, Ph.D. dissertation, Texas A&M University, College Station, TX, 1990

Zimmerman, W., D.B. Bukur and S. Ledakowicz, *Chem. Eng. Sci.*, 47, 2707 (1992)

Table 1. Process conditions and mass balances used for kinetic parameter estimation.

	MB#	TOS	T	P	H_2/CO	SV
		h	°C	bar	(-)	NL/g-Fe/h
SB-21903	I/1	71-78	260	15	0.67	4.0
	I/2	94-101	260	15	0.67	1.7
	I/3	119-126	260	15	0.67	9.2
	I/4	152-164	240	15	0.67	2.0
	I/5	193-215	240	15	0.67	1.0
	I/6	225-238	240	15	0.67	5.5
	I/7	263-270	260	15	0.67	4.0
	I/8	298-310	240	15	2	4.2
	I/10	364-368	240	15	2	10.8
	I/13	489-505	260	15	0.67	4.0
	I/14	600-606	260	22.5	0.67	6.1
	I/15	647-654	260	22.5	0.67	1.0
SB-26203	II/1	86-92	260	15	2	7.1
	II/2	118-122	260	15	2	10.1
	II/3	142-146	260	15	2	23.5
	II/4	175-191	240	15	2	5.8
	II/5	224-240	260	25	0.67	6.7
	II/6	264-268	260	25	0.67	17.1
	II/7	297-313	260	25	0.67	2.0
SB-28603	III/1	94-101	220	15	0.67	4.1
	III/2	128-143	220	15	0.67	0.5
	III/3	166-170	220	15	2	9.5
	III/4	192-198	220	15	2	0.6
	III/5	224-238	260	8	2	1.5
	III/6	262-268	260	8	2	9.0
	III/7	287-292	240	8	0.67	5.5
	III/8	313-318	240	8	0.67	0.7

Table 2. Estimated values of kinetic parameters (ALII Model of Lox and Froment).

Parameter	**units**	**220°C**	**240°C**	**260°C**
(a) Weighting factors equal to 1				
$k_{CO,HC}$	mmol/kg/s/bar	0.277	1.46	4.02
$k_{t,p}$	mmol/kg/s/bar	0.151	0.0352	0.131
$k_{t,o}$	mmol/kg/s	-0.618	0.00644	-0.166
$k_v^{'}$	mmol/kg/s/bar^1.5	8.04	0.817	25.2
K_v	bar^-0.5	23.6	0.7	9.35
(b) Weighting factors from equation (4)				
$k_{CO,HC}$	mmol/kg/s/bar	0.0709	0.39	1.55
$k_{t,p}$	mmol/kg/s/bar	0.00463	0.016	0.0434
$k_{t,o}$	mmol/kg/s	0.0194	0.031	0.051
$k_v^{'}$	mmol/kg/s/bar^1.5	0.194	0.53	9.08
K_v	bar^-0.5	1.31	0.533	7.05

Table 3. Confidence intervals for kinetic parameters (ALII Model of Lox and Froment).

T = 220 ℃	***units***	***Parameter estimate***	***95%-confidence limit***	
			lower	***upper***
$k_{CO,HC}$	mmol/kg/s/bar	0.0709	0.0561	0.0856
$k_{t,p}$	mmol/kg/s/bar	0.00463	0.00365	0.00562
$k_{t,o}$	mmol/kg/s	0.0194	0.0143	0.0245
$k_{\nu}^{'}$	mmol/kg/s/bar^1.5	0.194	-0.401	0.79
K_{ν}	bar^-0.5	1.31	-4.34	6.97

T = 240 ℃	***units***	***Parameter estimate***	***95%-confidence limit***	
			lower	***upper***
$k_{CO,HC}$	mmol/kg/s/bar	0.391	0.324	0.459
$k_{t,p}$	mmol/kg/s/bar	0.016	0.0138	0.0182
$k_{t,o}$	mmol/kg/s	0.0305	0.023	0.038
$k_{\nu}^{'}$	mmol/kg/s/bar^1.5	0.531	-1.06	2.12
K_{ν}	bar^-0.5	0.533	-4.2	5.27

T = 260 ℃	***units***	***Parameter estimate***	***95%-confidence limit***	
			lower	***upper***
$k_{CO,HC}$	mmol/kg/s/bar	1.55	1.28	1.81
$k_{t,p}$	mmol/kg/s/bar	0.0434	0.0384	0.0484
$k_{t,o}$	mmol/kg/s	0.051	0.0286	0.0733
$k_{\nu}^{'}$	mmol/kg/s/bar^1.5	9.08	-43.8	62
K_{ν}	bar^-0.5	7.05	-20.1	34.2

Table 4. Activation energies and statistical parameters for the FTS and WGS reactions

		Standard Error	*t Stat*	*Lower 95%*	*Upper 95%*
$E_{\mathrm{CO,HC}}$	168.73	6.62	25.49	84.62	252.85
$E_{\mathrm{t,p}}$	122.41	4.89	25.05	60.33	184.50
$E_{\mathrm{t,o}}$	52.75	3.13	16.84	12.96	92.55
E_v	208.78	62.51	3.34	-585.46	1003.02

Table 5. Activation energies for the FTS and WGS reactions from the literature (in kJ/mol)

Author(s), Year	**Reactor**	**Catalyst**	**Paraffin formation**	**Olefin formation**	**WGS**	**Overall FT**
Yang *et al*., 2003	Fixed bed	Fe/Mn	97 – methane 111 – C_2^+	97	58	
Wang *et al*., 2003	Fixed bed	Fe/Cu/K	93 – methane 87 – C_2^+	111	45	
Lox and Froment, 1993	Fixed bed	Fe	94	132	28	
Zimmerman and Bukur, 1990	Slurry	Fe/Cu/K			132 – 137	86
Deckwer *et al*., 1986	Slurry	Fe/K			63 – 105	
Dictor and Bell, 1986	Slurry	Reduced and Unreduced Fe and Fe/K	80 – 90*	100 – 110*		105 (Fe/K), 109 (Fe)
Feimer *et al*., 1981	Fixed bed	$Fe/Cu/K_2O$	92 – CH_4 84 – C_2H_6 78 (C_2 – C_5 HC)		124	
Dry *et al*., 1972	Fixed bed differential	$Fe/K_2O/Al_2O_3/SiO_2$	70 (C_2 – C_5 HC **)			70

*as reported by Yang *et al*., 2003

**as reported by Feimer *et al*., 1981

Table 6.Kinetic parameters for WGS results obtained by the LM and LS methods (Yang et al. Model)

ID		units	initial guess	estimates	st. dev.	| t-value |	95% confidence interval low	high			
	$k_{v,0}$	mol g^{-1} s^{-1} $bar^{-1.5}$	0.1	22.86	393.7	0.05808	-791.5	837.2	**F-value**	**Corr. Coeff.**	**Iteration No.**
W04	E_v	kJ mol^{-1}	1	**61.15**	69.54	0.8793	-82.71	205	49.11	0.6377	255
	$K_{v,0}$	$bar^{-0.5}$	0.1	8.73E-08	1.80E-06	0.04847	-3.64E-06	3.81E-06	**MARR**	**SSQ**	**exitflag**
	ΔH_v	kJ mol^{-1}	1	**-80.87**	71.47	1.132	-228.7	66.97	20.72	1.52	1
	$k_{v,0}$	mol g^{-1} s^{-1} $bar^{-1.5}$	39800	39810	7586000	0.005248	-15650000	15730000	**F-value**	**Corr. Coeff.**	**Iteration No.**
W07	E_v	kJ mol^{-1}	90.7	**90.55**	844.5	0.1072	-1656	1838	59.17	0.9115	131
	$K_{v,0}$	$bar^{-0.5}$	0.0022	0.0001878	0.03676	0.005109	-0.07585	0.07623	**MARR**	**SSQ**	**exitflag**
	ΔH_v	kJ mol^{-1}	-39	**-49.9**	867.5	0.05752	-1844	1745	26.32	216.05	1
	$k_{v,0}$	mol g^{-1} s^{-1} $bar^{-1.5}$	39800	3.98E+04	1.15E+06	0.03473	-2.33E+06	2.41E+06	**F-value**	**Corr. Coeff.**	**Iteration No.**
W08	E_v	kJ mol^{-1}	90.7	**94.38**	127.2	0.7422	-168.7	357.4	32.2	0.6433	51
	$K_{v,0}$	$bar^{-0.5}$	0.0022	0.0002082	0.006362	0.03272	-0.01295	0.01337	**MARR**	**SSQ**	**exitflag**
	ΔH_v	kJ mol^{-1}	-39	**-46.21**	135	0.3424	-325.4	233	20.17	1.51	1

Table 7. Kinetic parameters for the WGS reaction obtained using the genetic algorithm followed by the LM or LS method

ID		units	initial guess	estimates	st. dev.	| t-value |	95% confidence interval low	95% confidence interval high			
	$k_{v,0}$	mol g^{-1} s^{-1} $bar^{-1.5}$		2.6E+09					**F-value**	**Corr. Coeff.**	
W17	E_v	kJ mol^{-1}		144.5							**GA**
	$K_{v,0}$	$bar^{-0.5}$		5.38					**MARR**	**SSQ**	
	ΔH_v	kJ mol^{-1}		0.0276					19.92		
	$k_{v,0}$	mol g^{-1} s^{-1} $bar^{-1.5}$	2.6E+09	2.64E+09	4.91E+09	0.5366	-7.52E+09	1.28E+10	**F-value**	**Corr. Coeff.**	
W18	E_v	kJ mol^{-1}	144.5	**143.5**	23.22	6.183	**95.52**	**191.6**	33.02	0.6509	**LM**
	$K_{v,0}$	$bar^{-0.5}$	5.38	3.32E+01	8.89E+02	0.03731	-1805	1872	**MARR**	**SSQ**	
	ΔH_v	kJ mol^{-1}	0.0276	**6.876**	120.3	0.05715	-242	255.8	20.089	276.5	
	$k_{v,0}$	mol g^{-1} s^{-1} $bar^{-1.5}$	2.6E+09	2.64E+09	2.38E+08	11.06	2.14E+09	3.13E+09	**F-value**	**Corr. Coeff.**	
W19	E_v	kJ mol^{-1}	144.5	**143.5**	23.21	6.185	**95.52**	**191.5**	33.19	0.6525	**LS**
	$K_{v,0}$	$bar^{-0.5}$	5.38	3.11E+01	8.34E+02	0.03726	-1695	1757	**MARR**	**SSQ**	
	ΔH_v	kJ mol^{-1}	0.0276	**6.58**	121	0.05439	-243.7	256.8	20.06	275.7	
	$k_{v,0}$	mol g^{-1} s^{-1} $bar^{-1.5}$		7.9E+07					**F-value**	**Corr. Coeff.**	
W20	E_v	kJ mol^{-1}		128.6							**GA**
	$K_{v,0}$	$bar^{-0.5}$		0.36					**MARR**	**SSQ**	
	ΔH_v	kJ mol^{-1}		-12.45					19.81		
	$k_{v,0}$	mol g^{-1} s^{-1} $bar^{-1.5}$	7.9E+07	7.92E+07	9.67E+08	0.0819	-1.92E+09	2.08E+09	**F-value**	**Corr. Coeff.**	
W21	E_v	kJ mol^{-1}	128.6	**128.1**	54.48	2.351	**15.36**	**240.8**	32.75	0.6489	**LM**
	$K_{v,0}$	$bar^{-0.5}$	0.36	7.08E-01	2.12E+01	0.03336	-43.22	44.64	**MARR**	**SSQ**	
	ΔH_v	kJ mol^{-1}	-12.45	**-10.12**	130.3	0.07768	-279.6	259.4	20.05	277.8	

Table 8. Kinetic parameters of FTS reaction by the LS method (Yang et al. Model)

							95% confidence interval		
ID		**units**	**initial guess**	**estimates**	**st. dev.**	**| t-value |**	**low**	**high**	**Fitting stat.**
	$k_{5,0}$	mol g^{-1} s^{-1} bar^{-1}	1.23E+04	12300	22750	0.5409	-32340	56940	
Fr02	E_5	kJ mol^{-1}	93.73	**91.97**	7.965	11.55	**76.34**	**107.6**	**F-value**
	$k_{7m,0}$	mol g^{-1} s^{-1} bar^{-1}	2.01E+06	2010000	6305000	0.3188	-10360000	14380000	14.9
	E_{7m}	kJ mol^{-1}	88.83	**108.7**	13.52	8.038	**82.13**	**135.2**	**MARR**
	$k_{7,0}$	mol g^{-1} s^{-1} bar^{-1}	1.10E+06	1100000	3228000	0.3408	-5234000	7434000	65.14
	E_7	kJ mol^{-1}	115.9	**111.4**	12.76	8.737	**86.42**	**136.5**	**SSQ**
	$k_8^{+},_0$	mol g^{-1} s^{-1}	0.006231	0.08758	0.08836	0.9911	-0.08581	0.261	29.67
	E_8^{+}	kJ mol^{-1}	54.7	**54.22**	4.294	12.63	**45.8**	**62.65**	**Corr. Coeff.**
	$k_8^{-},_0$	mol g^{-1} s^{-1} bar^{-1}	7.16E-02	0.01459	0.06998	0.2085	-0.1227	0.1519	0.1491
	E_8^{-}	kJ mol^{-1}	37.98	**44.03**	20.63	2.134	**3.544**	**84.52**	
	$K_{1,0}$	bar^{-1}	2.59	0.1877	0.4341	0.4325	-0.664	1.04	**Note**
	ΔH_1	J mol^{-1}	8.00E-09	157.6	9801	0.01608	-19070	19390	first 9 parameters as well as adsorption constants ($K_{X,0}$) are from Yang 2003
	$K_{2,0}$	bar^{-1}	0.00167	2.22E-02	0.01684	1.319	-0.01083	0.05526	
	ΔH_2	J mol^{-1}	8.00E-09	165.6	6269	0.02642	-12140	12470	
	$K_{3,0}$	-	8.34E-02	1.69E+00	3.247	0.5204	-4.682	8.062	
	ΔH_3	J mol^{-1}	8.00E-09	10.9	10180	0.001071	-19960	19980	
	$K_{4,0}$	bar^{-1}	1.21	0.05296	0.2267	2.34E-01	-0.3919	0.4978	
	ΔH_4	J mol^{-1}	8.00E-09	155.3	17730	8.76E-03	-34630	34940	
	$K_{6,0}$	-	0.1	0.4757	2.051	2.32E-01	-3.549	4.501	
	ΔH_6	J mol^{-1}	8.00E-09	5.576	18020	3.09E-04	-35360	35370	

Table 9. Kinetic parameters of Van der Laan and Beenackers Model ($\kappa_{t,p}^{(1)}$, $\kappa_{t,p}^{(2)}$, $\kappa_{r,o}^{(2)}$ and c treated as constant at a given temperature)

No.	κ_1	κ_p	$\kappa_{t,p}^{(1)}$	$\kappa_{t,p}^{(2)}$	$\kappa_{t,o}$	$\kappa_{r,o}^{(2)}$	$\kappa_{r,o}$	c
Temperature	220	C						
1	0.5531	19.43			30.51		2.215	
2	0.2176	12.02	3.804	0.8671	15.78	3.378	1.015	0.2011
3	0.9924	7.299			9.815		0.9276	
4	0.3314	9.712			6.414		0.777	
				MARR				
				32				
Temperature	240	C						
5	0.7768	8.729			3.073		-0.1939	
6	0.6468	11.81			9.628		0.3722	
7	0.5077	9.594			-0.07769		-0.2594	
8	2.609	9.399	5.151	1.699	5.265	4.819	0.1566	0.2734
9	3.562	9.689			9.245		0.6549	
10	3.58	12.06			6.552		0.3536	
11	0.9152	61.21			26.82		0.8048	
12	0.1449	26.35			-0.465		-0.266	
				MARR				
				41.6				
Temperature	260	C						
13	2.687	22.1			255		21.2	
14	1.899	15.15			62.64		7.077	
15	3.939	25.73			376.4		29.56	
16	2.645	20.72			245.3		21.9	
17	2.599	20.88			223.6		19.17	
18	3.547	26.92			312.8		25.24	
19	1.484	15.69			11.7		1.184	
20	6.479	11.79	7.032	1.921	62.36	120.2	11.91	0.1883
21	8.048	13.53			86.7		13.75	
22	12.04	13.68			155.6		20.71	
23	3.698	23.81			314.3		23.15	
24	6.123	26.89			340.6		23.25	
25	1.716	21.38			181.8		14.32	
26	1.493	7.933			7.244		1.369	
27	3.237	11.52			171.1		19.04	
				MARR				
				21.5				

Table 10. Kinetic parameters of Van der Laan and Beenackers Model ($\kappa_{t,p}^{(1)}$, $\kappa_{t,p}^{(2)}$ and c treated as constant at a given temperature)

No.	κ_1	κ_p	$\kappa_{t,p}^{(1)}$	$\kappa_{t,p}^{(2)}$	$\kappa_{t,o}$	$\kappa_{r,o}^{(2)}$	$\kappa_{r,o}$	c
Temperature	220	C						
1	0.5666	19.81			129.1	17.47	10.26	
2	0.2228	12.23	3.861	0.8901	39.17	10.12	3.024	0.199
3	0.9814	7.325			6.846	2.113	0.5506	
4	0.3451	9.853			19.26	14.58	2.849	
				MARR				
				31.7				
Temperature	240	C						
5	0.9106	21			10.49	2.528	0.4768	
6	0.6581	11.79			39.36	25.96	2.899	
7	1.35	21.02			13.75	2.827	0.7281	
8	2.604	9.284	5.106	1.671	6.311	6.1	0.3143	0.2281
9	3.593	9.634			137.1	91.19	16.8	
10	3.591	11.91			13.02	11.05	1.23	
11	0.7475	45.96			7.27	0.6098	0.2728	
12	0.3304	33.18			33.94	9.369	1.808	
				MARR				
				24.7				
Temperature	260	C						
13	2.679	22.16			39.62	17.45	2.769	
14	1.888	15.12			19.02	33.53	1.768	
15	3.924	25.77			41.52	12.19	2.73	
16	2.629	20.69			32.44	14.73	2.407	
17	2.572	20.73			27.87	13.82	1.947	
18	3.299	24.68			10.27	3.078	0.5611	
19	1.493	15.58			7.056	11.9	0.5615	
20	6.49	11.83	7.013	1.912	19.81	36.61	3.247	0.2009
21	8.073	13.61			26.5	35.26	3.619	
22	12.22	13.9			214.2	163.1	25.89	
23	3.747	24.51			165.9	60.96	10.9	
24	5.835	24.75			14.77	4.422	0.6987	
25	1.66	20.49			16.02	9.465	0.926	
26	1.499	7.945			4.873	27.1	0.7514	
27	3.27	11.66			380.3	263.9	39.32	
				MARR				
				21.1				

Table 11. t-values of parameters obtained with $\kappa_{t,p}^{(1)}$, $\kappa_{t,p}^{(2)}$ and c as constant

No.	κ_1	κ_p	$\kappa_{t,p}^{(1)}$	$\kappa_{t,p}^{(2)}$	$\kappa_{t,o}$	$\kappa_{r,o}^{(2)}$	$\kappa_{r,o}$	c
Temperature	220	C						
1	19.5	11.6			0.084	0.080	0.079	
2	7.53	5.28	15	6.15	0.20	0.18	0.17	3.83
3	31	20			1.58	1.05	0.76	
4	11.4	10.3			0.26	0.24	0.22	
Temperature	220	C						
5	14.5	9.14			1.83	1.32	1.20	
6	9.78	6.89			0.28	0.27	0.25	
7	21.2	13			1.72	1.31	1.17	
8	38.6	27.7	35.7	20.5	4.51	3.12	1.96	10.6
9	52.1	35.2			0.13	0.13	0.12	
10	52.7	40.1			1.57	1.38	1.10	
11	10.3	4.54			1.84	0.81	1.20	
12	5.07	2.51			0.28	0.26	0.26	
Temperature	220	C						
13	18	11.4			0.63	0.60	0.57	
14	12.4	9.68			0.66	0.56	0.57	
15	26.6	15.1			0.84	0.78	0.74	
16	17.6	11.5			0.69	0.65	0.62	
17	17.3	11.4			0.83	0.77	0.72	
18	23	13.8			2.64	1.97	1.83	
19	10.1	7.95			1.23	0.72	0.92	
20	41.9	34.2	50.9	25.8	0.83	0.79	0.73	17
21	52.2	40.9			0.86	0.82	0.76	
22	78.3	54.5			0.14	0.14	0.14	
23	25.2	14.7			0.22	0.22	0.21	
24	40.2	23.5			3.45	2.75	2.22	
25	11.3	7.56			1.05	0.89	0.83	
26	9.79	7.45			0.73	0.35	0.55	
27	21.2	14.7			0.05	0.05	0.05	

Table 12. Improved values of kinetic parameters for Van der Laan and Beenackers Model

No.	MB#	κ_i	κ_p	$\kappa_{t,p}^{(1)}$	$\kappa_{t,p}^{(2)}$	$b^{(2)}$	b	c
Temperature 220°C								
1	28603-001	0.53	18.8	3.80	0.85	5.97	9.8	0.171
2	28603-002	0.22	11.9			3.03	9.8	
3	28603-003	0.98	7.2			1.98	6.3	
4	28603-004	0.34	9.7			1.07	5.0	
MARR for 220°C								
31.0								
Temperature 240°C								
5	21903-004	1.02	21.8	4.75	1.66	5.11	11.9	0.194
6	21903-005	0.68	11.5			2.22	10.0	
7	21903-006	1.50	21.2			6.16	11.3	
8	21903-008	2.78	9.3			1.33	8.4	
9	21903-010	3.70	9.5			2.38	6.4	
10	26203-004	3.72	11.7			1.76	6.9	
11	28603-007	0.89	51.9			8.98	13.5	
12	28603-008	0.34	31.7			5.36	12.6	
MARR for 240°C								
24.8								
Temperature 260°C								
13	21903-001	2.89	22.2	6.52	1.91	4.07	11.7	0.186
14	21903-002	1.94	15.0			0.93	8.3	
15	21903-003	4.32	25.9			6.05	12.4	
16	21903-007	2.84	20.8			3.90	10.9	
17	21903-013	2.77	20.9			3.53	11.3	
18	21903-014	3.83	27.0			5.02	12.0	
19	21903-015	1.61	16.3			0.91	8.0	
20	26203-001	6.65	11.7			1.03	5.0	
21	26203-002	8.33	13.5			1.42	6.1	
22	26203-003	12.75	13.7			2.43	7.3	
23	26203-005	4.01	23.9			4.91	13.2	
24	26203-006	6.64	27.0			5.41	14.2	
25	26203-007	1.81	21.4			2.85	12.2	
26	28603-005	1.54	7.9			0.23	4.2	
27	28603-006	3.46	11.7			2.68	8.7	
MARR for 260°C								
21.3								

Table 13. t-values of improved kinetic parameters

No.	MB name	κ_i	κ_p	$\kappa_{t,p}^{(1)}$	$\kappa_{t,p}^{(2)}$	$b^{(2)}$	b	c
Temperature 220°C								
1	28603-001	18.9	13.0	14.5	6.2	7.6	7.5	13
2	28603-002	8.0	5.4			2.6	4.1	
3	28603-003	27.0	20.3			10.4	10.9	
4	28603-004	13.3	10.6			1.9	5.8	
Temperature 240°C								
5	21903-004	16.3	10.0	35	20	4.6	8.8	35
6	21903-005	9.8	6.9			2.3	5.1	
7	21903-006	23.3	14.2			7.6	11.4	
8	21903-008	37.8	27.0			7.0	16.9	
9	21903-010	47.7	36.2			14.3	18.2	
10	26203-004	50.4	41.5			10.7	19.0	
11	28603-007	15.1	4.9			3.5	8.2	
12	28603-008	6.1	2.9			1.3	3.6	
Temperature 260°C								
13	21903-001	19.6	13.1	49	26	4.7	11.2	57
14	21903-002	12.8	10.5			1.2	7.8	
15	21903-003	29.3	17.7			8.3	15.7	
16	21903-007	19.2	13.2			4.7	11.0	
17	21903-013	18.7	13.0			4.2	10.8	
18	21903-014	26.8	16.0			6.5	14.9	
19	21903-015	10.9	8.9			0.9	6.9	
20	26203-001	43.3	35.8			5.1	19.3	
21	26203-002	53.1	43.4			7.8	23.6	
22	26203-003	72.2	57.6			17.9	29.1	
23	26203-005	26.7	17.2			7.1	14.6	
24	26203-006	42.9	26.6			11.7	21.5	
25	26203-007	12.2	8.6			2.3	7.4	
26	28603-005	9.8	7.4			0.4	4.0	
27	28603-006	21.6	15.1			5.4	10.1	

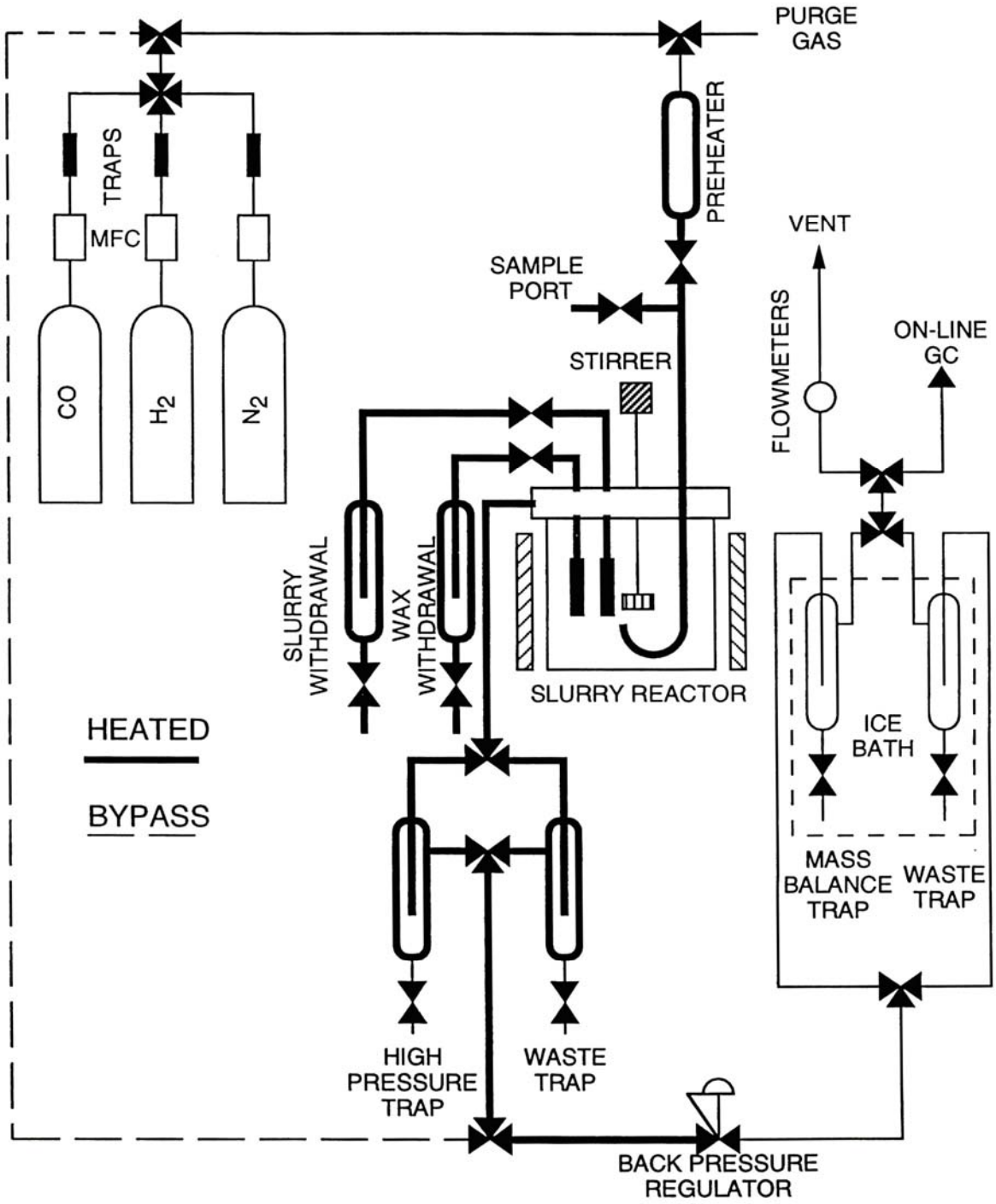

Figure 1. Schematic of stirred tank slurry reactor system.

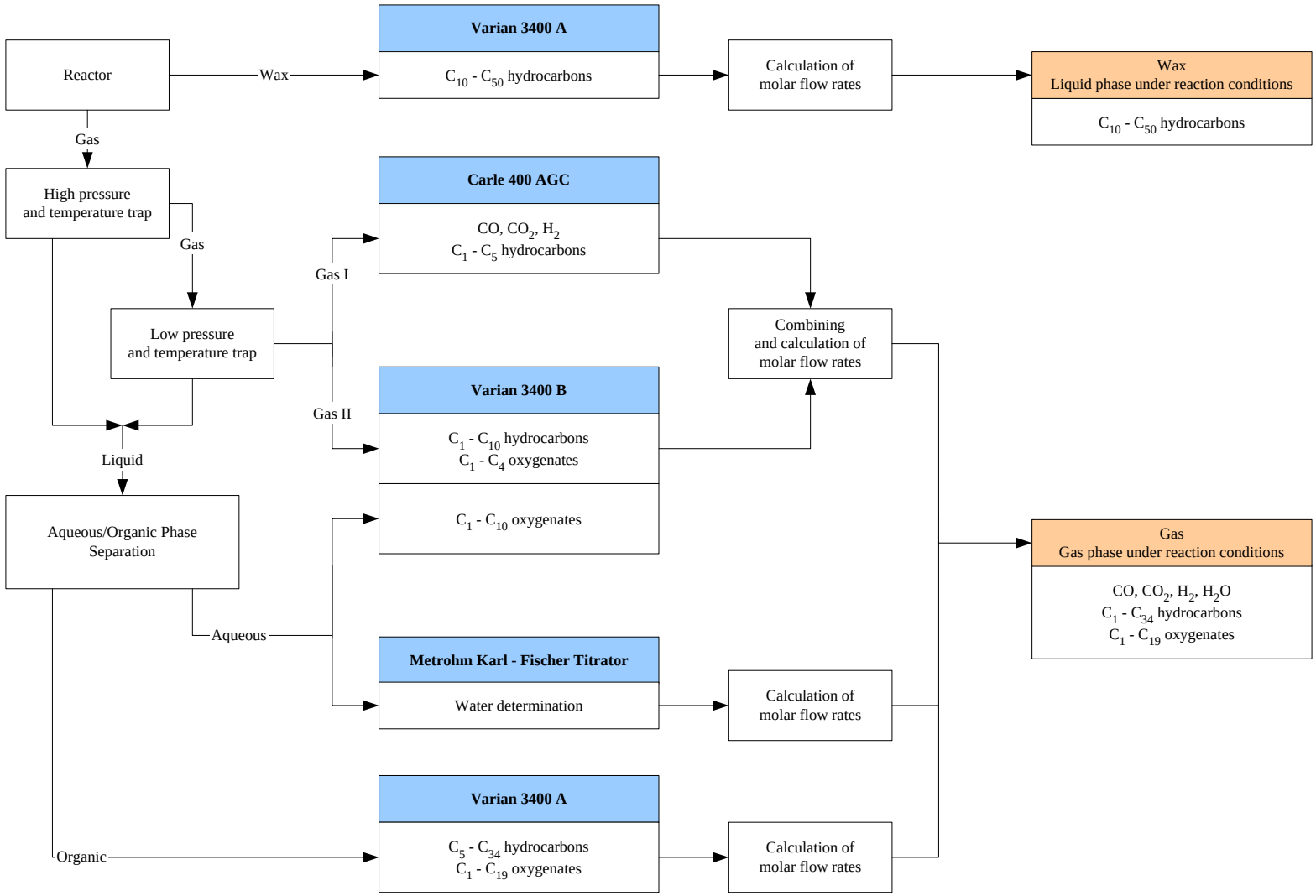

Figure 2. Product analysis schematic.

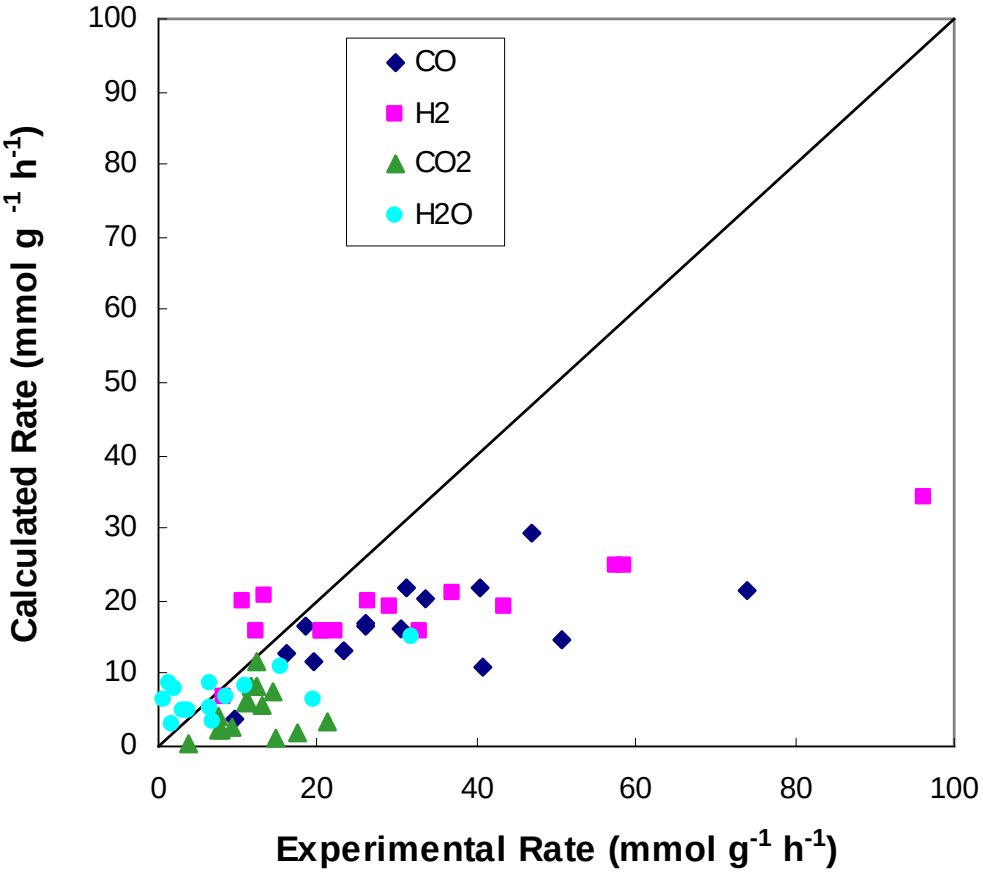

Figure 3. Parity graph of experimental and calculated reaction rates at 260 ℃ for H_2, CO, CO_2 and H_2O.

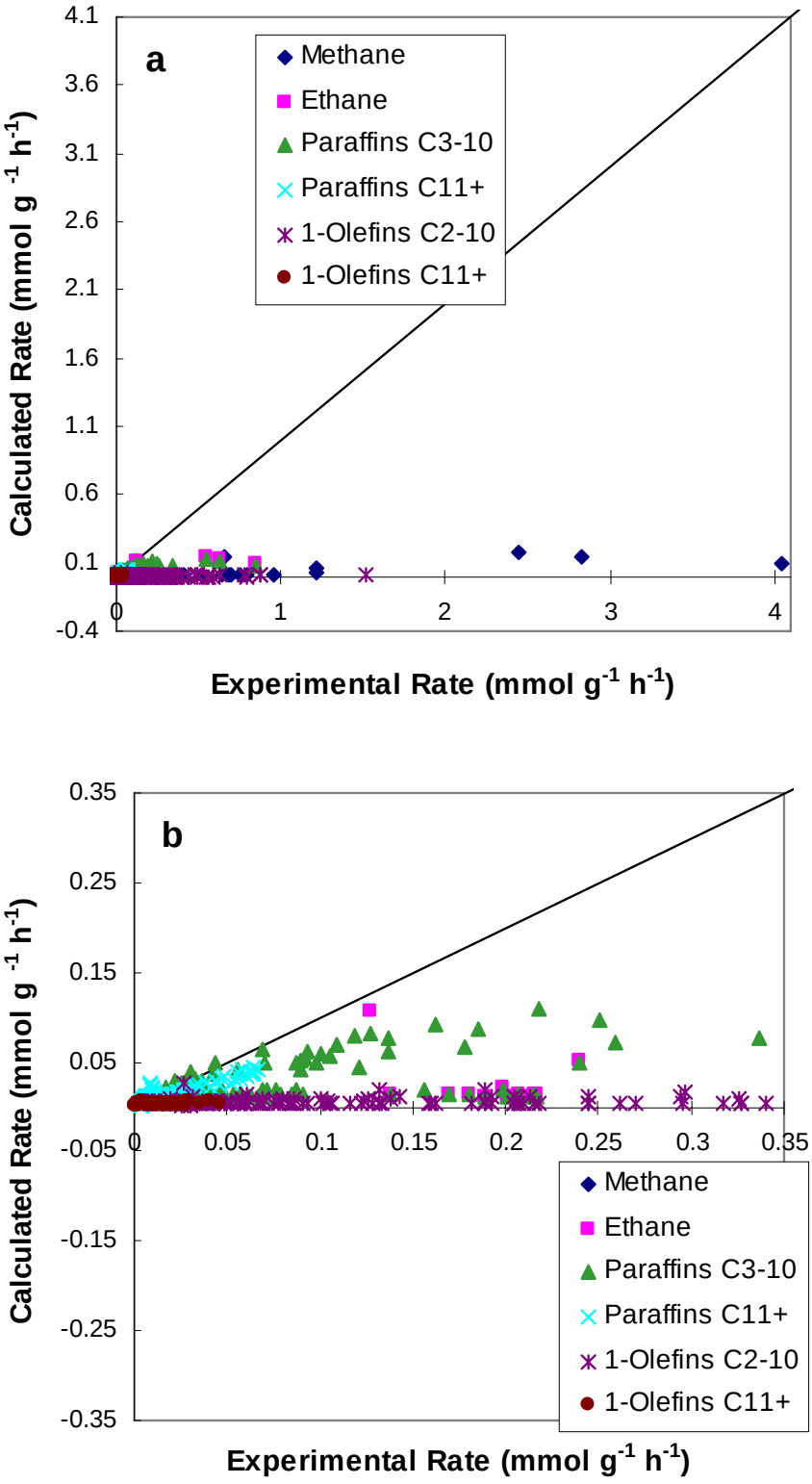

Figure 4. Parity graph of experimental and calculated reaction rates at *260℃* for hydrocarbons.

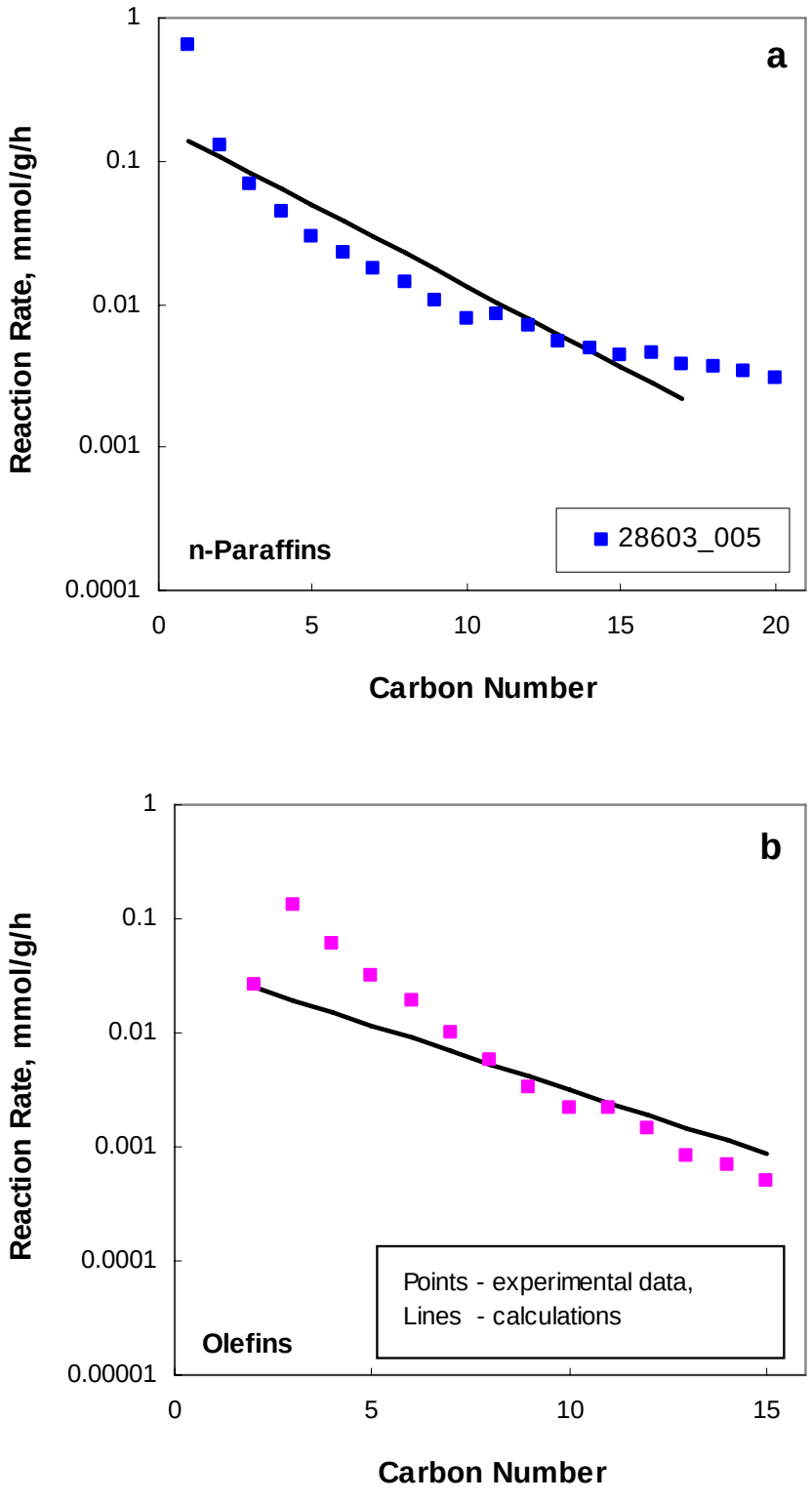

Figure 5. Comparison of experimental data and model predictions for n-paraffins and total olefins at T = 260°C, 8 bar, $H_2/CO = 2$, SV = 1.45 Nl/g_{Fe}/h.

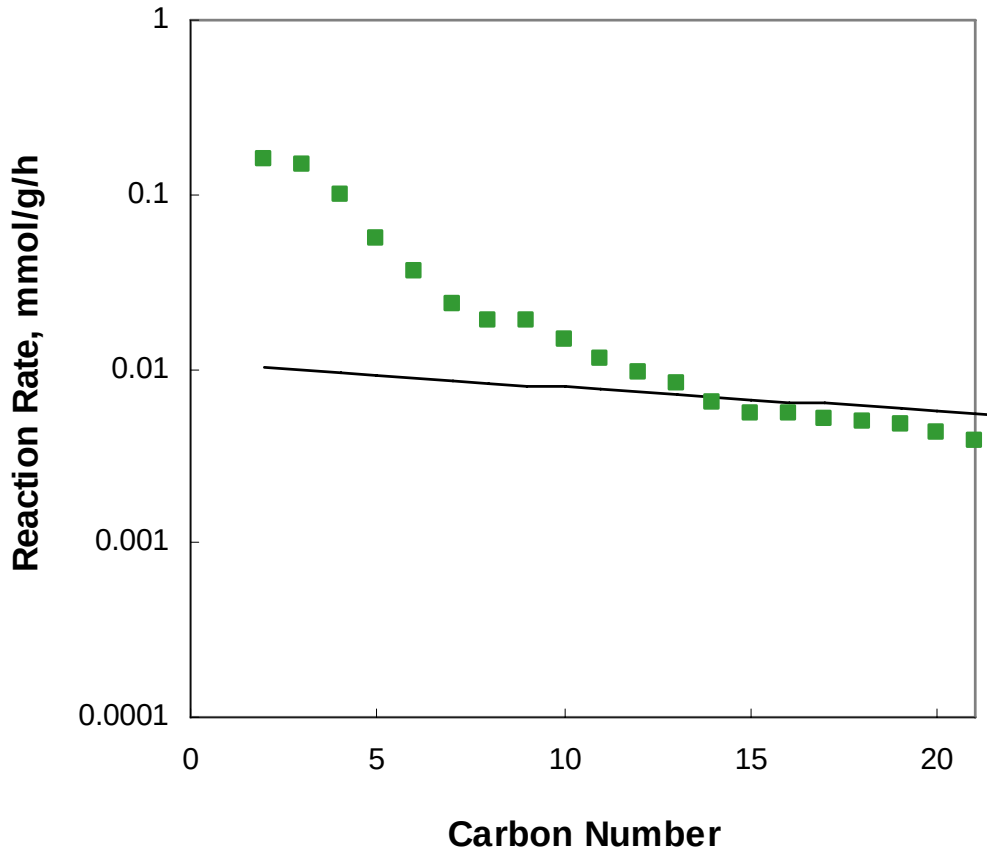

Figure 6. Carbon number distribution of hydrocarbon products - Comparison of model predictions with experimental data (Reaction conditions: T = 240°C, 15 bar, H_2/CO = 2/3, SV = 2.0 $Nl/g_{Fe}/h$).

.

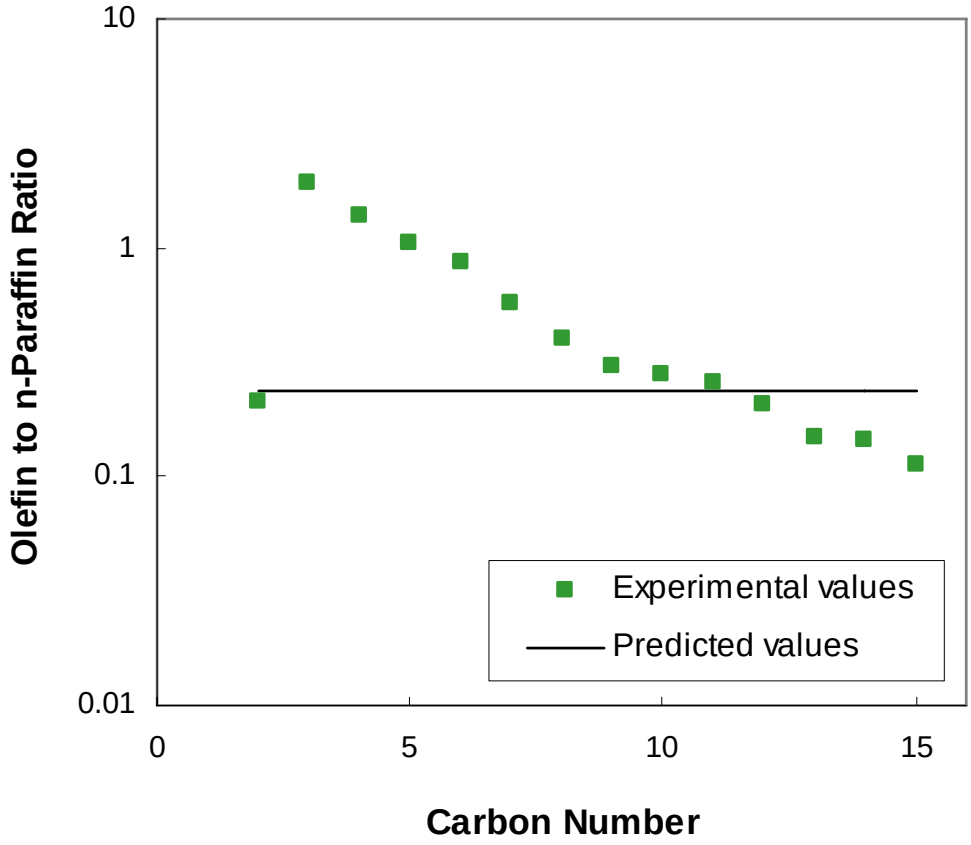

Figure 7. Olefin to paraffin ratio change with carbon number – Comparison of model predictions with experimental data (Reaction conditions: T = 260°C, 8 bar, $H_2/CO = 2$, SV = 1.45 $Nl/g_{Fe}/h$.

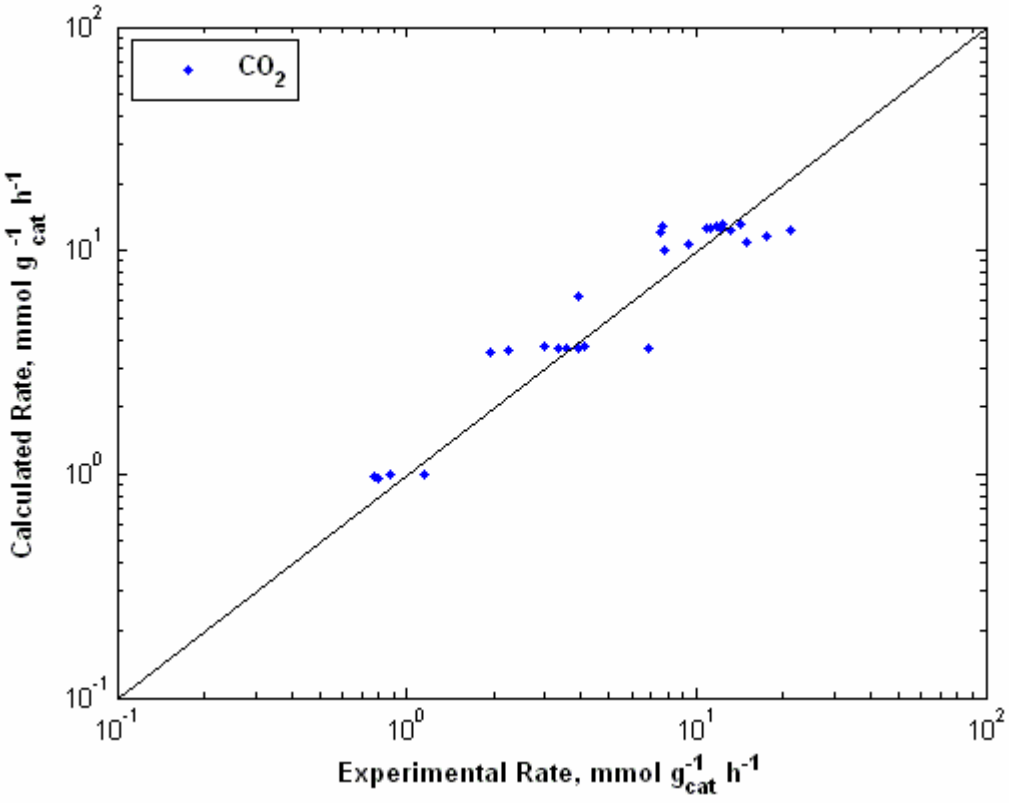

Figure 8. Parity plot for carbon dioxide formation rate (LS Method).

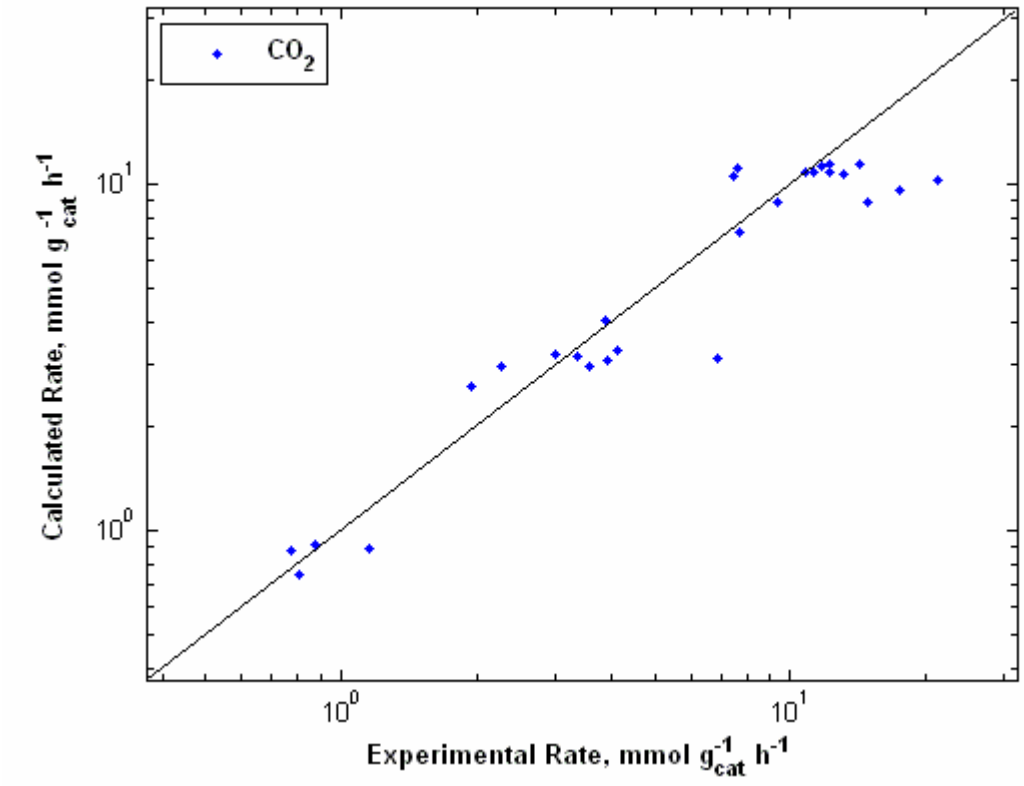

Figure 9. Parity plot for carbon dioxide (GA method followed by LM method).

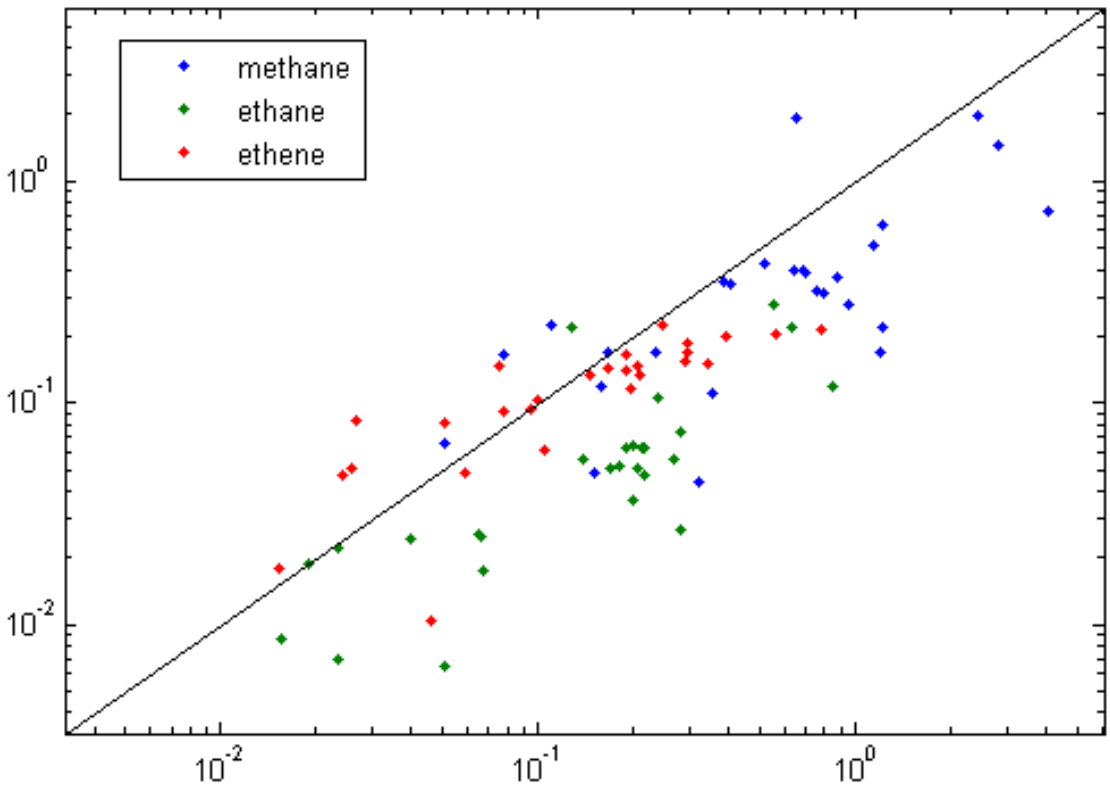

Figure 10. Parity plot for low molecular weight hydrocarbons (Yang et al. Model).

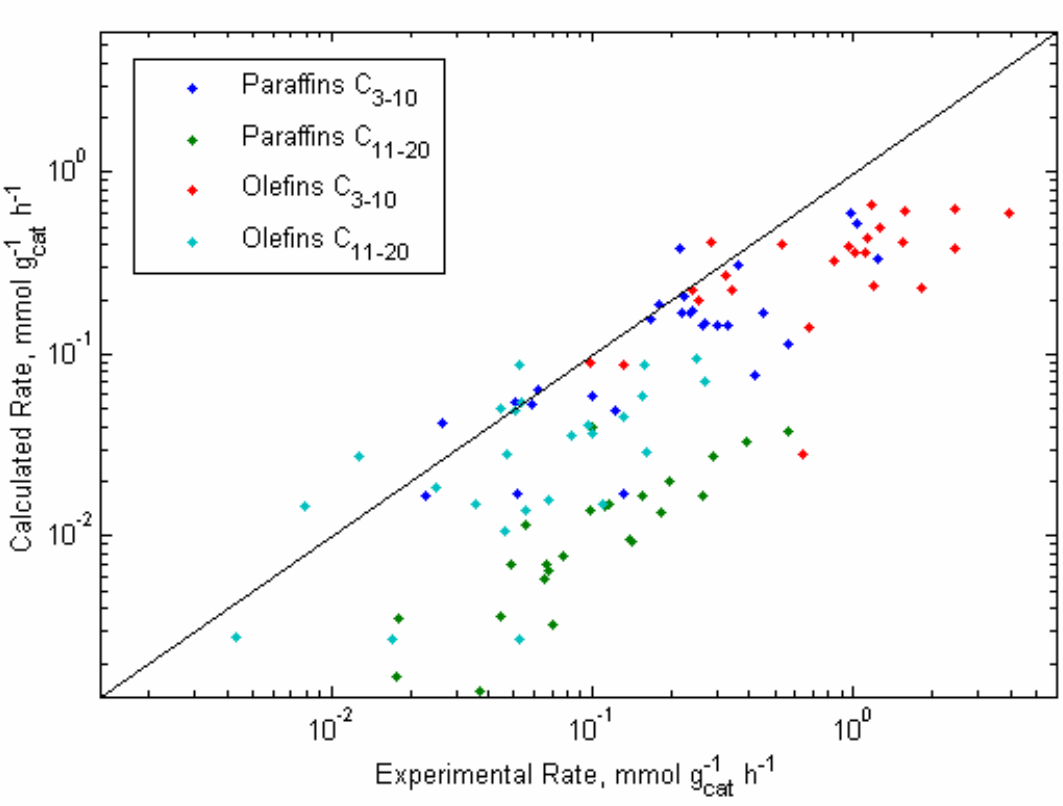

Figure 11. Parity plot for higher molecular weight hydrocarbons (Yang et al. Model).

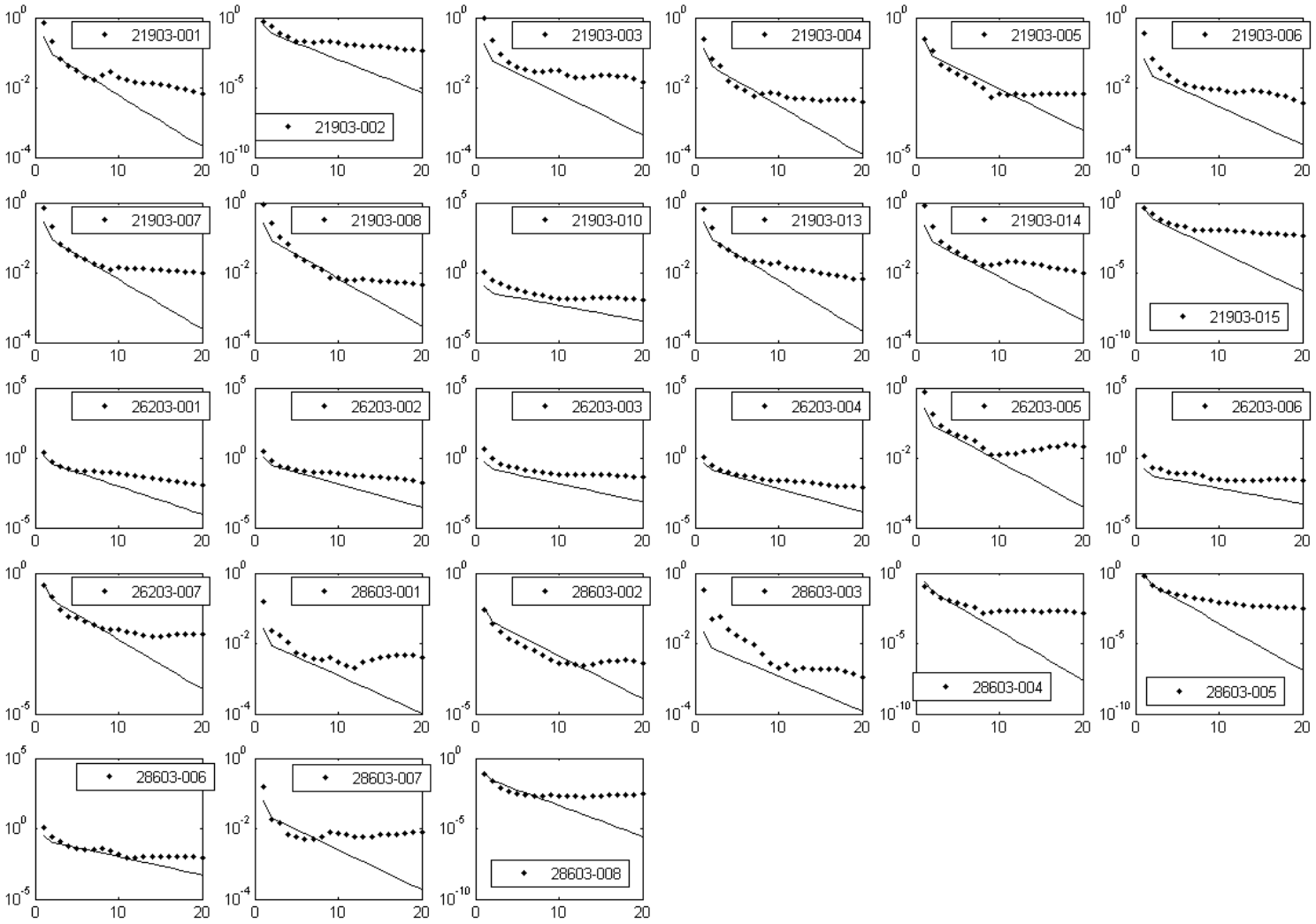

Figure 12. Comparison of experimental data and model predictions for n-paraffins.

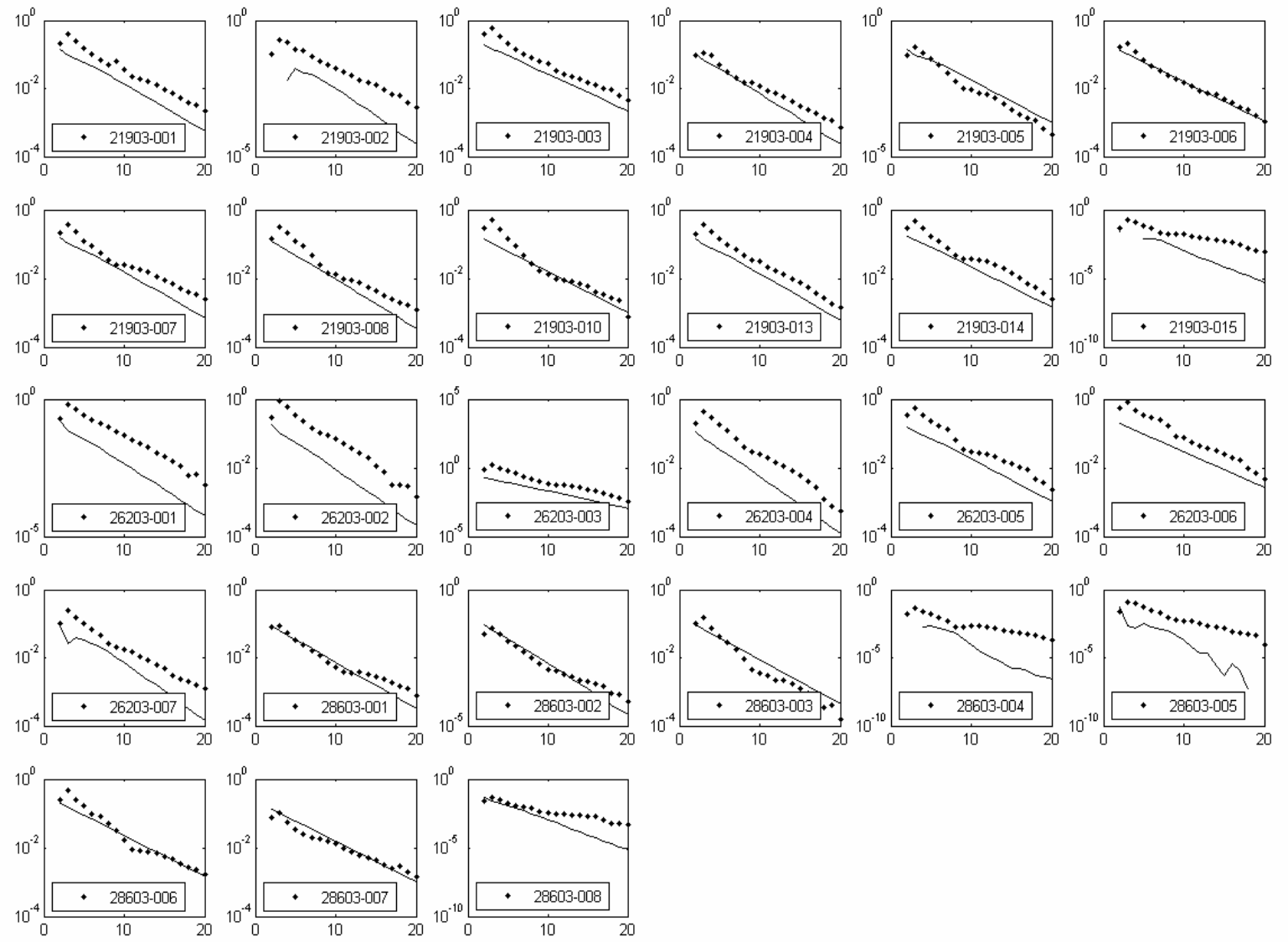

Figure 13. Comparison of experimental data and model predictions for linear olefins.

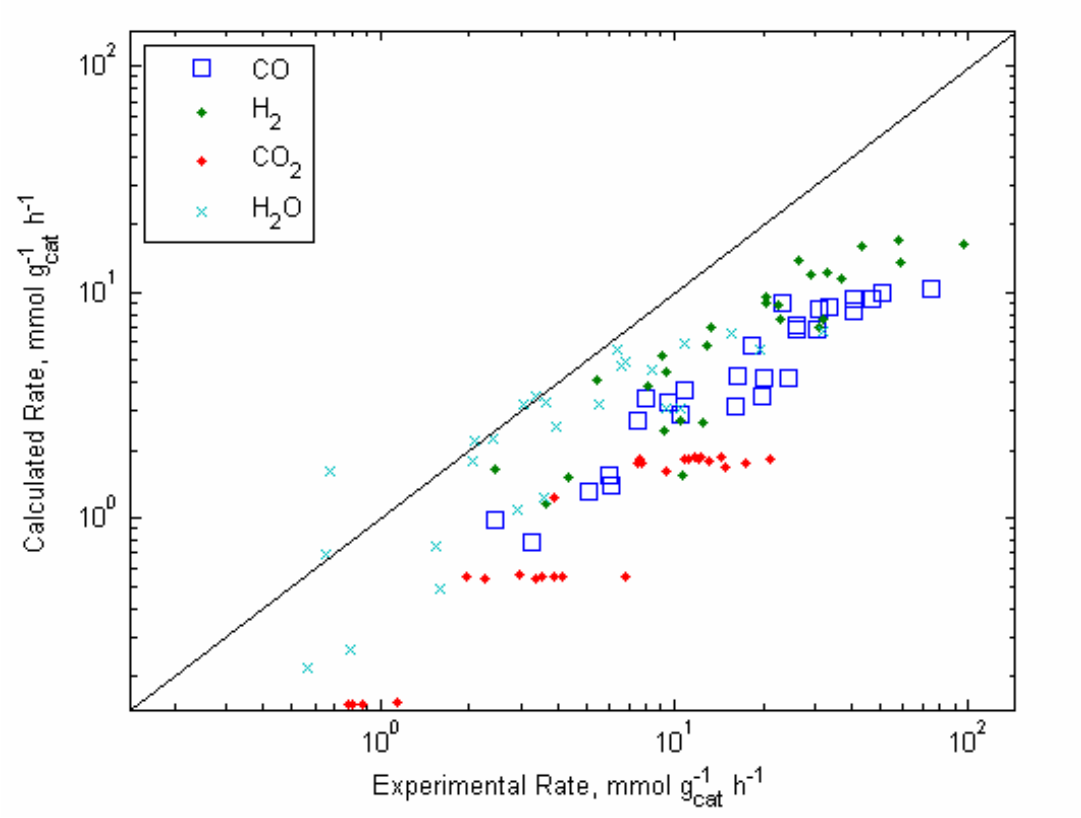

Figure 14. Parity plot for inorganic species (Yang et al. 2003).

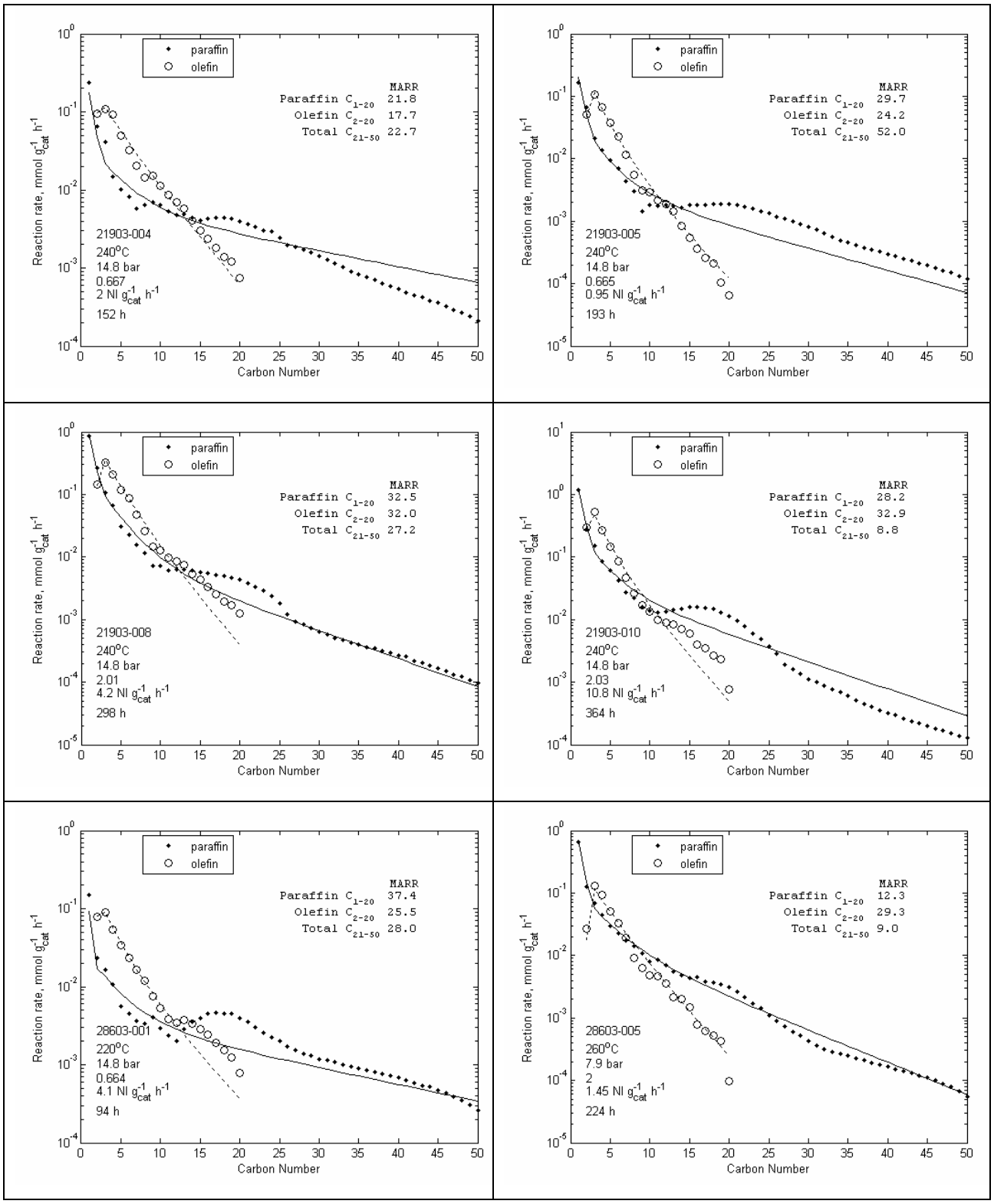

Figure 15. Comparison of predicted and experimental product distributions (Van der Laan and Beenackers Model)

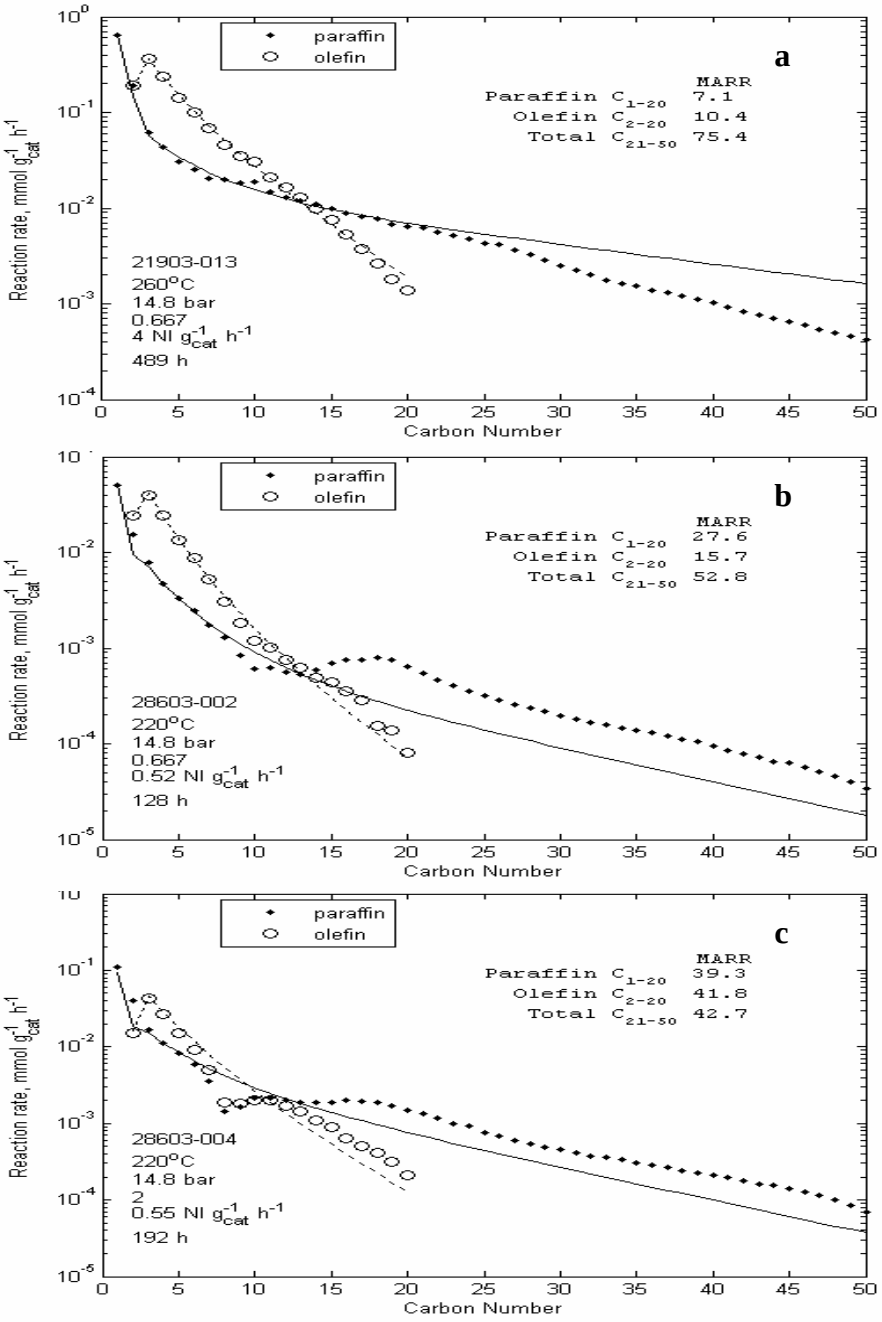

Figure 16. Comparison of predicted and experimental product distributions (a) Best, (b) median and (c) worst total MARR.

Appendix A Lox and Froment's Model

ALII model of Lox and Froment (1993b) utilizes Langmuir-Hinshelwood-Hougen-Watson (LHHW) approach and concept of the rate-determining steps (RDS). Elementary steps (reactions) for Fischer-Tropsch synthesis (FTS) and Water-Gas-Shift (WGS) reaction are shown in Tables A-1 and A-2, respectively. Reactant molecules are adsorbed on two types of active sites, one for FTS and the second for WGS reaction, where the surface reactions take place. The model assumes two RDS in each path of formation of paraffins and olefins in the Fischer-Tropsch reaction:

- adsorption of carbon monoxide (HC1) and desorption of the paraffin (HC5) in the reaction path leading to the paraffins,
- adsorption of carbon monoxide (HC1) and desorption of the olefin (HC6) in the reaction path leading to the olefins,

Table A-1. Elementary reactions for FTS (ALII Model in Lox and Froment, 1993b).

No.	Elementary reactions	Expression of rates and equilibrium constants
HC1	$CO + C_{n-1}H_{2n-1}l_1 \rightarrow C_{n-1}H_{2n-1}l_1CO \quad (n \geq 1)$	$k_{HC1}\ (k_{CO})$
HC 2	$C_{n-1}H_{2n-1}l_1CO + H_2 = C_{n-1}H_{2n-1}l_1C + H_2O \ (n \geq 1)$	K_{HC2}
HC 3	$C_{n-1}H_{2n-1}l_1C + H_2 = C_{n-1}H_{2n-1}l_1CH_2 \ (n \geq 1)$	K_{HC3}
HC 4	$C_{n-1}H_{2n-1}l_1CH_2 = C_nH_{2n+1}l_1 \quad (n \geq 1)$	K_{HC4}
HC 5	$C_nH_{2n+1}l_1 + H_2 \rightarrow C_nH_{2n+2} + Hl_1 \quad (n \geq 1)$	$k_{\mathrm{HC5}}\ (k_{\mathrm{t,p}})$
HC 6	$C_nH_{2n+1}l_1 \rightarrow C_nH_{2n} + Hl_1 \quad (n \geq 2)$	$k_{\mathrm{HC6}}\ (k_{\mathrm{t,o}})$
HC 7	$H_2 + 2l_1 = 2Hl_1$	$K_{\mathrm{HC7}}\ (K_{\mathrm{H_2}})$

where l_1 means a vacant active site on the surface of catalyst.

Assumptions:

- Elementary reactions 2,3,4,7 are in pseudo equilibrium. Steps 1, 5 and 6 are not at equilibrium (irreversible steps).
- There is no single rate-determining step.
- Reactions proceed according to Hougen-Watson (H-W) mechanism.
- Reactant molecules are absorbed at active sites onto the surface of the catalyst

The above mechanism gives following rates for particular components (concentrations expressed in mol/m^3):

Paraffin rates:

$$R_{C_nH_{2n+2}} = \frac{k_{t,p} \cdot C_{H_2} \cdot \frac{k_{CO,HC} \cdot C_{CO}}{k_{CO,HC} \cdot C_{CO} + k_{t,p} \cdot C_{H_2}} \cdot (\alpha)^{n-1}}{1 + \frac{k_{CO,HC} \cdot C_{CO}}{k_{CO,HC} \cdot C_{CO} + k_{t,p} \cdot C_{H_2}} \cdot \frac{1}{1-\alpha}} \quad n \geq 1 \tag{A.1}$$

Olefin rates:

$$R_{C_nH_{2n}} = \frac{k_{t,o} \cdot \frac{k_{CO,HC} \cdot C_{CO}}{k_{CO,HC} \cdot C_{CO} + k_{t,p} \cdot C_{H_2}} \cdot (\alpha)^{n-1}}{1 + \frac{k_{CO,HC} \cdot C_{CO}}{k_{CO,HC} \cdot C_{CO} + k_{t,p} \cdot C_{H_2}} \cdot \frac{1}{1-\alpha}} \quad n \geq 2 \tag{A.2}$$

where

$$\alpha = \frac{k_{CO,HC} \cdot C_{CO}}{k_{CO,HC} \cdot C_{CO} + k_{t,p} \cdot C_{H_2} + k_{t,o}} \tag{A.3}$$

$$\left\langle k_{CO,HC} \right\rangle = \frac{1}{s \cdot g_{cat}} \cdot m^3 \qquad \left\langle k_{t,p} \right\rangle = \frac{1}{s \cdot g_{cat}} \cdot m^3 \qquad \left\langle k_{t,o} \right\rangle = \frac{1}{s \cdot g_{cat}} \cdot mol$$

These parameters correspond to k_1, k_5 and k_6, respectively, in Table IX (Lox and Froment, 1993b).

The following WGS mechanism was used. The RDS for the WGS reaction is a reaction between adsorbed carbon monoxide and adsorbed hydroxyl group (WGS2 in Table A-2).

Table A-2. Elementary reactions for WGS (ALII Model in Lox and Froment, 1993b).

No.	Elementary reactions	Expression of rates (small) and equilibrium constants (capital letter)
WGS1	$CO + l_2 = COl_2$	$K_{1,WGS}$
WGS2	$COl_2 + OHl_2 = COOHl_2 + l_2$	$k_{2,WGS}$, $K_{2,WGS}$
WGS3	$COOHl_2 = CO_2 + Hl_2$	$K_{3,WGS}$
WGS4	$H_2O + 2 \cdot l_2 = OHl_2 + Hl_2$	$K_{4,WGS}$
WGS5	$H_2 + 2 \cdot l_2 = 2 \cdot Hl_2$	$K_{5,WGS}$

where l_2 is a vacant active site on the surface of catalyst, but different type than l_1 (in Table A-1)

Rate of carbon dioxide formation is given by:

$$R_{CO_2} = \frac{k_v^{'} \cdot \left(C_{H_2O} \cdot C_{CO} \big/ {C_{H_2}}^{0.5} - \frac{1}{K_{WGS}} \cdot C_{CO_2} \cdot {C_{H_2}}^{0.5} \right)}{\left(1 + K_v \cdot C_{H_2O} \big/ {C_{H_2}}^{0.5} \right)^2} \qquad \text{(A.4)}$$

where

$$k_v^{'} = k_{2,WGS} \cdot \frac{K_{CO,WGS} \cdot K_{H_2O,WGS}}{{K_{H_2,WGS}}^{0.5}} \cdot {C_{l_2,tot}}^2 \qquad \left\langle k_v^{'} \right\rangle = \frac{mol}{s \cdot g_{cat}} \cdot \left(\frac{m^3}{mol} \right)^{1.5}$$

$$K_v = \frac{K_{H_2O,WGS}}{{K_{H_2,WGS}}^{0.5}} \qquad \left\langle k_v^{'} \right\rangle = \left(\frac{m^3}{mol} \right)^{-0.5}$$

These parameters correspond to k_v and K_v parameters in Table IX (Lox and Froment, 1993b).

The equilibrium constant of water gas shift reaction K_{WGS} is a function of temperature only (Lox and Froment, 1993b)

$$\ln(K_{WGS}) = 5078.0045 \cdot T^{-1} - 5.8972089 + 13.958689 \cdot 10^{-4} \cdot T + - 27.592844 \cdot 10^{-8} \cdot T^{2} \quad \text{(A.5)}$$

If one assumes that the only products are n-paraffins, linear olefins, carbon dioxide and water, then the rates of formation of CO, H_2, and water can be expressed from the reaction stoichiometry as:

Carbon monoxide

$$R_{CO} = \sum_{n=1}^{50}\left(\frac{-n}{1} \cdot R_{C_nH_{2n+2}}\right) + \sum_{n=2}^{50}\left(\frac{-n}{1} \cdot R_{C_nH_{2n}}\right) + \frac{-1}{1} R_{CO_2} \quad \text{(A.6)}$$

Hydrogen

$$R_{H_2} = \sum_{n=1}^{50}\left(\frac{-2n-1}{1} \cdot R_{C_nH_{2n+2}}\right) + \sum_{n=2}^{50}\left(\frac{-2n}{1} \cdot R_{C_nH_{2n}}\right) + \frac{1}{1} \cdot R_{CO_2} \quad \text{(A.7)}$$

Water

$$R_{H_2O} = \sum_{n=1}^{50}\left(\frac{n}{1} \cdot R_{C_nH_{2n+2}}\right) + \sum_{n=2}^{50}\left(\frac{n}{1} \cdot R_{C_nH_{2n}}\right) + \frac{-1}{1} R_{CO_2} \quad \text{(A.8)}$$

Note that rates of formation of H_2 and CO will be negative. Also, this model predicts that rates of formation of n-paraffins and olefins, as well as the chain growth probability factor, are independent of carbon number (Equations A.1-A.3). This model predicts that the olefin to paraffin ratio is independent of carbon number, and that the carbon number distribution follows the ideal Schulz-Flory distribution.

Appendix B Kinetic Model of Li and co-workers

Main features of kinetic model of Yang et al. (2003) are:

- olefin readsorption,
- different kinetic rate constant for methane than for others paraffins,
- solution of hydrocarbon formation reaction rates requires numerical solution of a set of two non-linear algebraic equations,
- olefin to paraffin ratio is a function of carbon number.

Hydrocarbon Formation

Elementary reactions for this model are given in Table B-1.

Table B-1. Elementary steps of FTS (FTIII in Yang et al., 2003).

No.	Elementary reactions	Expression of rates (small) and equilibrium constants (capital letter)
HC1	$CO + l_1 \rightarrow COl_1$	$K_{HC1}\ (K_{CO})$
HC 2	$COl_1 + H_2 = H_2COl_1$	K_{HC2}
HC 3	$H_2COl_1 + H_2 = CH_2\,l_1 + H_2O$	$K_{HC3}\ (K_{H_2O})$
HC 4	$H_2 + 2l_1 = 2Hl_1$	$K_{HC4}\ (K_{H_2})$
HC 5(n)	$CH_2\,l_1 + CH_2\,l_1 = CH_2CH_2\,l_1 + l_1$ $C_nH_{2n}\,l_1 + CH_2\,l_1 = C_nH_{2n}CH_2\,l_1 + l_1$ $n \geq 1$	$k_{HC5}\ (k_p)$
HC 6(n)	$C_nH_{2n}\,l_1 + H\,l_1 = C_nH_{2n+1}\,l_1 + l_1$ $n \geq 1$	K_{HC6}
HC 7(n)	$C_nH_{2n+1}\,l_1 + H\,l_1 \rightarrow C_nH_{2n+2} + 2l_1$ $n \geq 1$	$k_{HC7M}\ (k_{t,CH_4})$ $k_{HC7}\ (k_{t,p})$
HC 8(n)	$C_nH_{2n}\,l_1 = C_nH_{2n} + l_1$ $n \geq 2$	$k^{+}_{HC8},\ k^{-}_{HC8},\ (K_{t,o})$

where l_1 means a vacant active site on the surface of catalyst.

Assumptions:

- Steps HC5, 7 and 8 are RDS. All other elementary reactions are in dynamic equilibrium;
- Steady-state conditions are reached for both the surface composition of catalyst and concentrations of all of surface intermediates involved;
- Rate constant of elementary steps for formation of hydrocarbons ($k_{t,p}$) is independent of carbon number of the intermediate involved in the elementary reaction except for methane (k_{t,CH_4});
- Reactant molecules are absorbed at active sites onto the surface of the catalyst.

Rates of formation of methane, other paraffins and olefins are given in Equations B-1, B-2 and B-3, respectively. Methane rate constant (k_{HC7M}) is different than rate constants for other paraffins (k_{HC7}).

$$R_{CH_4} = k_{HC7M} \cdot K_1 \cdot K_2 \cdot K_3 \cdot K_4 \cdot K_6 \cdot \frac{\hat{f}_{CO} \cdot \hat{f}_{H_2}^3}{\hat{f}_{H_2O}} \cdot \left(\frac{1}{DENOM}\right)^2 \tag{B.1}$$

$$R_{C_nH_{2n+2}} = k_{HC7} \cdot K_1 \cdot K_2 \cdot K_3 \cdot K_4 \cdot K_6 \cdot \frac{\hat{f}_{CO} \cdot \hat{f}_{H_2}^3}{\hat{f}_{H_2O}} \cdot \prod_{i=2}^{n} \alpha_i \cdot \left(\frac{1}{DENOM}\right)^2 \tag{B.2}$$

$n \geq 2$

$$R_{C_nH_{2n}} = k_{HC8}^{+} \cdot (1-\beta_n) \cdot K_1 \cdot K_2 \cdot K_3 \cdot \frac{\hat{f}_{CO} \cdot \hat{f}_{H_2}^2}{\hat{f}_{H_2O}} \cdot \frac{1}{DENOM} \cdot \prod_{i=2}^{n} \alpha_i \tag{B.3}$$

$n \geq 2$

where

$$\alpha_n = \frac{k_{HC5} \cdot A_1}{k_{HC5} \cdot A_1 + k_{HC7} \cdot A_2 + k_{HC8}^{+} \cdot (1-\beta_n) \cdot DENOM} \tag{B.4}$$

$n \geq 2$

$$\beta_n = \frac{k_{HC8}^{-}}{k_{HC8}^{+}} \cdot \frac{\hat{f}_{C_nH_{2n}}}{A_1 \cdot A^{n-1} + B \cdot \sum_{i=2}^{n} A^{i-2} \cdot \hat{f}_{C_{n-i+2}H_{2(n-i+2)}}} \tag{B.5}$$

$n \geq 2$

$$A = \frac{k_{HC5} \cdot A_1}{k_{HC5} \cdot A_1 + k_{HC7} \cdot A_2 + k_{HC8}^{+} \cdot DENOM} \tag{B.6}$$

$$B = \frac{k_{HC8}^{-} \cdot DENOM}{B_1 + k_{HC8}^{+} \cdot DENOM} \tag{B.7}$$

$$B_1 = k_{HC5} \cdot A_1 + k_{HC7} \cdot A_2 \tag{B.8}$$

$$A_1 = K_1 K_2 K_3 \cdot \frac{\hat{f}_{CO} \cdot \hat{f}_{H_2}^2}{\hat{f}_{H_2O}} \tag{B.9}$$

$$A_2 = K_4 K_6 \cdot \hat{f}_{H_2} \tag{B.10}$$

and DENOM is

$$\begin{aligned} DENOM = {} & 1 + K_4^{0.5} \cdot \hat{f}_{H_2}^{0.5} + K_1 \cdot \hat{f}_{CO} + A_1 + K_1 K_2 \cdot \hat{f}_{CO} \cdot \hat{f}_{H_2} + \\ & + K_1 \cdot K_2 \cdot K_3 \cdot K_4^{0.5} \cdot K_6 \cdot \frac{\hat{f}_{CO} \cdot \hat{f}_{H_2}^{2.5}}{\hat{f}_{H_2O}} + \\ & + A_1 \cdot \left(1 + K_4^{0.5} K_6 \cdot \hat{f}_{H_2}^{0.5}\right) \cdot \sum_{j=2}^{n} \prod_{i=2}^{j} \alpha_i \end{aligned} \tag{B.11}$$

WGS Reaction

Assumptions:

- Elementary reactions 1 – 3 and 5 (Table B-2) are in dynamic equilibrium. The 4th step is the rate-determining step (RDS);
- Reactant molecules are absorbed at active sites onto the surface of the catalyst.
- Concentrations of the adsorbed species involved in RDS reaction(s) are much larger then those of the other adsorbed species.

Table B-2. Elementary steps for WGS reaction (WGS3 in Yang et al., 2003).

No.	Elementary reactions	Expression of rates (small) and equilibrium constants (capital letter)
WGS1	$CO + l_2 = COl_2$	K_{WGS1}
WGS2	$H_2O + 2 \cdot l_2 = OHl_2 + Hl_2$	K_{WGS2}
WGS3	$COl_2 + OHl_2 = COOHl_2 + l_2$	K_{WGS3}
WGS4	$COOHl_2 = CO_2 + Hl_2$	k_{WGS4}, K_{WGS4}
WGS5	$2 \cdot Hl_2 = H_2 + 2 \cdot l_2$	$1/K_{WGS5}$

where l_2 means a vacant active site on the surface of catalyst, but different type than l_C.

The above mechanism leads to the following rate of carbon dioxide formation:

$$R_{CO_2} = k_V \cdot \left(\frac{\hat{f}_{CO} \cdot \hat{f}_{H_2O} - \frac{1}{K_{WGS}} \cdot \hat{f}_{CO_2} \cdot \hat{f}_{H_2}}{\hat{f}_{H_2}^{0.5} + K_V \cdot \hat{f}_{CO} \cdot \hat{f}_{H_2O}} \right) \tag{B.12}$$

where K_{WGS} is given by Equation (A.5) and

$$K_V = K_{WGS} \frac{K_{WGS5}^{0.5}}{K_{WGS4}} \tag{B.13}$$

$$k_V = k_{WGS4} K_{WGS} \tag{B.14}$$

Appendix C Hydrocarbon Selectivity Model of Van der Laan and Beenackers

Van der Laan and Beenackers (1998, 1999) developed olefin readsorption product distribution model (ORPDM) for formation of hydrocarbons in Fischer-Tropsch synthesis (FTS). Reaction network of hydrocarbon formation for this model is presented in Figure C-1. Chain growth is initiated by hydrogenation of adsorbed monomer ($^{*}CH_2$) to adsorbed methyl group ($^{*}CH_3$). Chain propagation occurs via insertion of adsorbed monomer into adsorbed alkyl species ($^{*}C_nH_{2n+1}$), which can terminate to paraffin (C_nH_{2n+2}) by hydrogenation or to olefin (C_nH_{2n}) by dehydrogenation (hydrogen abstraction). According to this reaction network olefin readsorbtion leads to adsorbed alkyl species, which can propagate or terminate. Detailed stoichiometry and kinetic equations of ORPDM model for its elementary reactions are presented in Table C-1.

ORPDM is selectivity model with pseudo-constants (λ), which include true kinetic constants (k) and concentrations of some intermediates. Van der Laan and Beenackers assumed that kinetic parameters (rate constant) for methane and ethylene formation are different than the corresponding rate constants for C_2^+ paraffins and C_3^+ olefins.

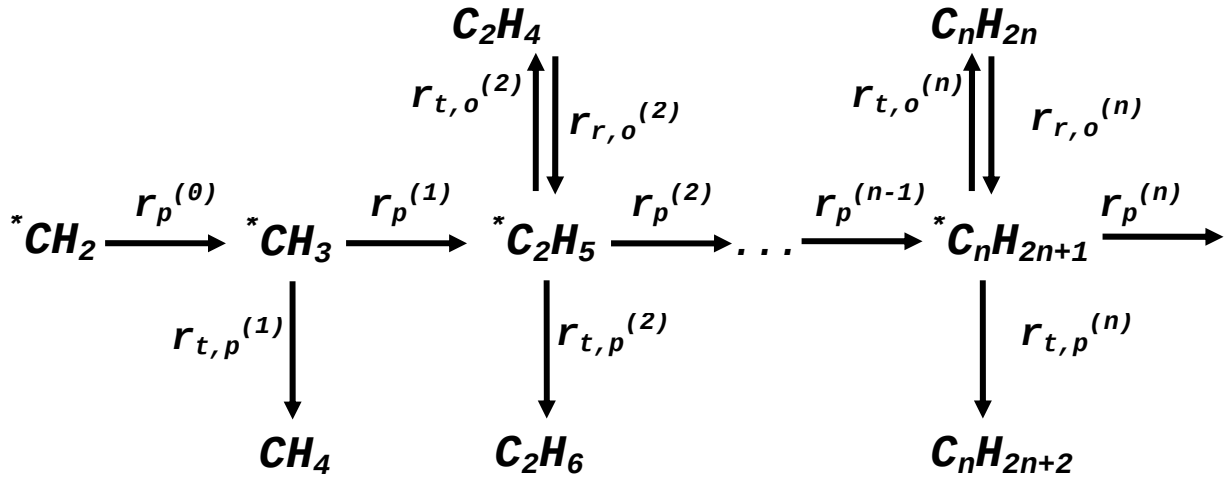

Figure C-1. Reaction network of hydrocarbon formation (FTS) with olefin readsorption.

Table C-1. Elementary steps of FTS (Van der Laan and Beenackers 1998)

No.	Stoichiometry equations	Kinetic equations
HC1	**formation of adsorbed methyl group C_1^*** $CH_2, s_1 + H, s_1 \xrightarrow{k_{p,1}} CH_3, s_1$	$r_p^{(0)} = k_{p,1} \cdot \theta_{CH_2,s_1} \cdot \theta_{H,s_1} = \lambda_1$
HC2	**propagation** $C_nH_{2n+1}, s_1 + CH_2, s_1 \xrightarrow{k_p} C_{n+1}H_{2n+3}, s_1$ $n = 1, 2, ...$	$r_p^{(n)} = k_p \cdot \theta_{CH_2,s_1} \cdot \theta_{C_nH_{2n+1},s_1}$ $r_p^{(n)} = \lambda_p \cdot \theta_{C_nH_{2n+1},s_1}$ *where* $\lambda_p = k_p \cdot \theta_{CH_2,s_1}$ $n = 1, 2, ...$
HC3	**termination to paraffin** $C_nH_{2n+1}, s_1 + H, s_1 \xrightarrow{k_{t,p}} C_nH_{2n+2} + 2s_1$ $n = 1, 2, ...$	$r_{t,p}^{(n)} = k_{t,p} \cdot \theta_{H,s_1} \cdot \theta_{C_nH_{2n+1},s_1}$ $r_{t,p}^{(n)} = \lambda_{t,p} \cdot \theta_{C_nH_{2n+1},s_1}$ *where* $\lambda_{t,p} = k_{t,p} \cdot \theta_{H,s_1}$ $n = 1, 2, ...$
HC4	**termination to olefin** $C_nH_{2n+1}, s_1 + s_1 \xrightarrow{k_{t,o}} C_nH_{2n} + H, s_1 + s_1$ $n = 2, 3, ...$	$r_{t,o}^{(n)} = k_{t,o} \cdot \theta_{s_1} \cdot \theta_{C_nH_{2n+1},s_1}$ $r_{t,o}^{(n)} = \lambda_{t,o} \cdot \theta_{C_nH_{2n+1},s_1}$ *where* $\lambda_{t,o} = k_{t,o} \cdot \theta_{s_1}$ $n = 2, 3, ...$
HC5	**olefin readsorption** $C_nH_{2n} + H, s_1 + s_1 \xrightarrow{k_{r,o}} C_nH_{2n+1}, s_1 + s_1$ $n = 2, 3, ...$	$r_{r,o}^{(n)} = k_{r,o} \cdot \theta_{s_1} \cdot \theta_{H,s_1} \cdot C^s_{C_nH_{2n}}$ $r_{r,o}^{(n)} = \lambda^*_{r,o} \cdot C^s_{C_nH_{2n}}$ *where* $\lambda^*_{r,o} = k_{r,o} \cdot \theta_{s_1} \cdot \theta_{H,s_1}$ $n = 2, 3, ...$

s_1 means an active site on the surface of catalyst; θ is a surface coverage of adsorbed species;

C^S is a concentration of species at the surface.

Based on reaction network shown in Figure C-1 and kinetic equations in Table C-1 the reaction rates for paraffin and olefin formation are:

Methane

$$R_{CH_4} = r_{t,p}^{(1)} = \lambda_{t,p}^{(1)} \cdot \theta_{CH_3,s_1} \tag{C.1}$$

Paraffin C_2^+

$$R_{C_nH_{2n+2}} = r_{t,p}^{(n)} = \lambda_{t,p} \cdot \theta_{C_nH_{2n+1},s_1} \tag{C.2}$$

Ethene

$$R_{C_2H_4} = r_{t,o}^{(2)} - r_{r,o}^{(2)} = \lambda_{t,o}^{(2)} \cdot \theta_{C_2H_5,s_1} - \lambda_{r,o}^{*(2)} \cdot C_{C_2H_4}^{s} \tag{C.3}$$

Olefin C_3^+

$$R_{C_nH_{2n}} = r_{t,o}^{(n)} - r_{r,o}^{(n)} = \lambda_{t,o} \cdot \theta_{C_nH_{2n+1},s_1} - \lambda_{r,o}^{*} \cdot C_{C_nH_{2n}}^{s} \tag{C.4}$$

where θ is a surface coverage of adsorbed species whereas C^S is a concentration of species at the surface. Both of them are unknown.

The assumption was made that the reaction rate of an olefin $R_{C_nH_{2n}}$ is proportional to its partial pressure $p_{C_nH_{2n}}$ in the gas phase of perfectly mixed continuous reactor, i.e.

$$R_{C_nH_{2n}} = p_{C_nH_{2n}} \cdot \frac{SV}{R_g \cdot T} \quad n \geq 2 \tag{C.5}$$

where R_g is a universal gas constant, T is temperature and SV is a space velocity ($m^3\, g_{cat}\, h^{-1}$) at the reactor exit.

Partial pressure $p_{C_nH_{2n}}$ and concentration $C_{C_nH_{2n}}^{s}$ of species at the surface are related by vapor-liquid equilibrium constant called pseudo-Henry constant $He_{C_nH_{2n}}$

$$p_{C_nH_{2n}} = C_{C_nH_{2n}}^{s} \cdot He_{C_nH_{2n}} \tag{C.6}$$

Equilibrium constant $He_{C_nH_{2n}}$ is an exponential function which depends upon the carbon number of the olefin

$$He_{C_nH_{2n}} = He_0 \cdot \exp(-c \cdot n) \tag{C.7}$$

where *c* is a positive constant.

Surface coverage of the intermediate species $\theta_{\theta_{C_nH_{2n+1},s_1}}$ can be calculated using the pseudo-steady state approximation:

$$\frac{d\theta_{\theta_{C_nH_{2n+1},s_1}}}{dt} = 0 \tag{C.8}$$

All the above equations and assumptions lead to the following expressions for reaction rates of hydrocarbons:

Methane

$$R_{CH_4} = \lambda_{t,p}^{(1)} \cdot \frac{\lambda_1}{\lambda_p + \lambda_{t,p}^{(1)}} \tag{C.9}$$

Ethane

$$R_{C_2H_6} = \lambda_{t,p}^{(2)} \cdot \frac{\lambda_1}{\lambda_p + \lambda_{t,p}^{(1)}} \cdot \alpha_2 \tag{C.10}$$

Paraffin C_3^+

$$R_{C_nH_{2n+2}} = \lambda_{t,p} \cdot \frac{\lambda_1}{\lambda_p + \lambda_{t,p}^{(1)}} \cdot \prod_{i=2}^{n} \alpha_i \tag{C.11}$$

Ethene

$$R_{C_2H_4} = \frac{\lambda_{t,o}^{(2)}}{1 + \lambda_{r,p}^{(2)} \cdot \exp(2c)} \cdot \frac{\lambda_1}{\lambda_p + \lambda_{t,p}^{(1)}} \cdot \alpha_2 \tag{C.12}$$

Olefin C_3^+

$$R_{C_nH_{2n}} = \frac{\lambda_{t,o}}{1 + \lambda_{r,o} \cdot \exp(c \cdot n)} \cdot \frac{\lambda_1}{\lambda_p + \lambda_{t,p}^{(1)}} \cdot \prod_{i=2}^{n} \alpha_i \tag{C.13}$$

Olefin to Paraffin ratio, from Equations (C.13) and (C.11), is

$$\frac{R_{C_nH_{2n}}}{R_{C_nH_{2n+2}}} = \frac{\lambda_{t,o}}{\lambda_{t,p} \cdot \left(1 + \lambda_{r,o} \cdot \exp(c \cdot n)\right)} \qquad n \geq 3 \tag{C.14}$$

Equations C.9 to C.14 contain 10 parameters ($\lambda_1, \lambda_p, \lambda_{t,p}^{(1)}, \lambda_{t,p}^{(2)}, \lambda_{t,p}, \lambda_{t,o}^{(2)}, \lambda_{t,o}, \lambda_{r,o}^{(2)}, \lambda_{r,o}, c$).

In order to reduce number of parameters the pseudo-constants (λ) are re-parameterized with reference to termination of paraffin ($\lambda_{t,p}$). Additionally termination to ethene is related to ethane and olefin terminations. This leads to relative pseudo-constants (κ)

$$R_{CH_4} = \kappa_{t,p}^{(1)} \cdot \frac{\kappa_1}{\kappa_p + \kappa_{t,p}^{(1)}} \tag{C.15}$$

$$R_{C_2H_6} = \kappa_{t,p}^{(2)} \cdot \frac{\kappa_1}{\kappa_p + \kappa_{t,p}^{(1)}} \cdot \alpha_2 \tag{C.16}$$

$$R_{C_nH_{2n+2}} = \frac{\kappa_1}{\kappa_p + \kappa_{t,p}^{(1)}} \cdot \prod_{i=2}^{n} \alpha_i \tag{C.17}$$

$n \geq 3$

$$R_{C_2H_4} = \frac{\kappa_{t,o}^{(2)}}{1 + \kappa_{r,o}^{(2)} \cdot \exp(2c)} \cdot \frac{\kappa_1}{\kappa_p + \kappa_{t,p}^{(1)}} \cdot \alpha_2 \tag{C.18}$$

$$R_{C_nH_{2n}} = \frac{\kappa_{t,o}}{1 + \kappa_{r,o} \cdot \exp(c \cdot n)} \cdot \frac{\kappa_1}{\kappa_p + \kappa_{t,p}^{(1)}} \cdot \prod_{i=2}^{n} \alpha_i \qquad n \geq 3 \tag{C.19}$$

Chain growth probability factor α can be calculated as:

$$\alpha_n = \frac{\kappa_p}{1 + \kappa_p + \dfrac{\kappa_{t,o}}{1 + \kappa_{r,o} \cdot \exp(c \cdot n)}} \qquad n \geq 3 \tag{C.20}$$

$$\alpha_2 = \frac{\kappa_p}{\kappa_{t,p}^{(2)} + \kappa_p + \dfrac{\kappa_{t,o}^{(2)}}{1 + \kappa_{r,o}^{(2)} \cdot \exp(2c)}} \tag{C.21}$$

where: $\kappa_1 = \lambda_1$,

$$\kappa_p = \lambda_p / \lambda_{t,p},$$

$$\kappa_{t,p}^{(1)} = \lambda_{t,p}^{(1)} / \lambda_{t,p},$$

$$\kappa_{t,p}^{(2)} = \lambda_{t,p}^{(2)} / \lambda_{t,p}, \qquad \text{(C.22)}$$

$$\kappa_{t,o} = \lambda_{t,o} / \lambda_{t,p},$$

$$\kappa_{r,o} = \lambda_{r,o},$$

$$\kappa_{t,o}^{(2)} = \kappa_{t,p}^{(2)} \cdot \kappa_{t,o}$$

In addition, strong correlation between parameter $\kappa_{t,o}$ and $\kappa_{r,o}$ occurs at high olefin readsorption rate ($\kappa_{r,o} \cdot \exp(c \cdot n) >> 1$). In such a case, estimation of these parameters should not be done separately, and instead $\kappa_{t,o} / \kappa_{r,o}$ ratio needs to be estimated as one parameter (Van der Laan and Beenackers, 1999). This leads to the following equations:

$$R_{C_2H_4} = b^{(2)} \cdot \exp(-2c) \cdot \frac{\kappa_1}{\kappa_p + \kappa_{t,p}^{(1)}} \cdot \alpha_2 \qquad \text{(C.23)}$$

$$R_{C_nH_{2n}} = b \cdot \exp(-c \cdot n) \cdot \frac{\kappa_1}{\kappa_p + \kappa_{t,p}^{(1)}} \cdot \prod_{i=2}^{n} \alpha_i \qquad n \geq 3 \qquad \text{(C.24)}$$

$$\alpha_2 = \frac{\kappa_p}{\kappa_{t,p}^{(2)} + \kappa_p + b^{(2)} \cdot \exp(-2c)} \qquad \text{(C.25)}$$

$$\alpha_n = \frac{\kappa_p}{1 + \kappa_p + b \cdot \exp(-c \cdot n)} \qquad n \geq 3 \qquad \text{(C.26)}$$

where

$$b = \frac{\kappa_{t,p}^{(2)} \cdot \kappa_{t,o}}{\kappa_{r,o}^{(2)}} \qquad \text{(C.26)}$$

$$b^{(2)} = \frac{\kappa_{t,o}}{\kappa_{r,o}} \qquad \text{(C.27)}$$

Then the meaning of parameters *b* is the following

$$b^{(2)} = \frac{k_{t,p}^{(2)} \cdot k_{t,o}}{k_{r,o}^{(2)} \cdot \left(k_{t,p}\right)^2 \cdot \theta_{H,s_1}^2 \cdot \frac{R_g \cdot T}{SV}} \tag{C.28}$$

$$b = \frac{k_{t,o}}{k_{r,o} \cdot k_{t,p} \cdot \theta_{H,s_1}^2 \cdot \frac{R_g \cdot T}{SV}} \tag{C.29}$$

These parameters include reaction rate constants (*k*) as well as surface coverage of adsorbed hydrogen, so they may be depend on the temperature as well as on the other process conditions (P, SV and/or H_2/CO feed ratio).